

5-2011

Cardiac abnormalities after transaortic constriction are worsened by changing glucose metabolism and benefited by repair of mitochondrial DNA.

Jianxun Wang 1969-
University of Louisville

Follow this and additional works at: <https://ir.library.louisville.edu/etd>

Recommended Citation

Wang, Jianxun 1969-, "Cardiac abnormalities after transaortic constriction are worsened by changing glucose metabolism and benefited by repair of mitochondrial DNA." (2011). *Electronic Theses and Dissertations*. Paper 1517.
<https://doi.org/10.18297/etd/1517>

This Doctoral Dissertation is brought to you for free and open access by ThinkIR: The University of Louisville's Institutional Repository. It has been accepted for inclusion in Electronic Theses and Dissertations by an authorized administrator of ThinkIR: The University of Louisville's Institutional Repository. This title appears here courtesy of the author, who has retained all other copyrights. For more information, please contact thinkir@louisville.edu.

CARDIAC ABNORMALITIES AFTER TRANSAORTIC CONSTRICTION ARE
WORSENER BY CHANGING GLUCOSE METABOLISM AND BENEFITED BY
REPAIR OF MITOCHONDRIAL DNA

By

Jianxun Wang
B.S., Lanzhou University of China, 1991
M.S., Sun Yat-Sen University of China, 1994
M.S., University of Louisville, 2007

A Dissertation
Submitted to the Faculty of the
Graduate School of the University of Louisville
In Partial Fulfillment of the Requirements
for the Degree of

Doctor of Philosophy

Department of Pharmacology and Toxicology
University of Louisville, School of Medicine
Louisville, Kentucky

May 2011

CARDIAC ABNORMALITIES AFTER TRANSAORTIC CONSTRICTION ARE
WORSENER BY CHANGING GLUCOSE METABOLISM AND BENEFITED BY
REPAIR OF MITOCHONDRIAL DNA

By

Jianxun Wang
B.S., Lanzhou University of China, 1991
M.S., Sun Yat-Sen University of China, 1994
M.S., University of Louisville, 2007

A Dissertation Approved on

March 31, 2011

by the following Dissertation Committee:

Paul N. Epstein, Ph.D.

David W. Hein, Ph.D.

William M. Pierce Jr., Ph.D.

Frederick W. Benz, Ph.D.

Stephen J. Winters, M.D.

ACKNOWLEDGMENTS

I would like to thank my mentor, Dr. Paul N. Epstein, for his guidance and patience. I would also like to thank the other committee members, Drs. David W. Hein, William M. Pierce, Frederick W. Benz and Stephen J. Winters, for their valuable suggestions and assistance of this project. I would also like to thank my wife, Qianwen Wang, for her support.

ABSTRACT

CARDIAC ABNORMALITIES AFTER TRANSAORTIC CONSTRICTION ARE WORSENER BY CHANGING GLUCOSE METABOLISM AND BENEFITED BY REPAIR OF MITOCHONDRIAL DNA

Jianxun Wang

April 1, 2011

Heart failure is a leading cause of morbidity and mortality in the USA. During the development of heart failure, many cardiac parameters change at the same time including fuel metabolism, oxidative stress and mitochondrial function. Each of these changes occurs in the context of multiple other abnormalities in the failing heart. This complexity makes it difficult to discern the importance of each of these parameters. In this dissertation changes in glucose metabolism and mitochondrial DNA repair have been targeted separately and specifically in the heart to test their roles in heart failure independently.

Abnormal glucose metabolism is always found in heart failure patients. During heart failure there is a significant increase in cardiac glycolysis. On the other hand,

diabetic patients, who are at increased risk of heart failure show the opposite change in glucose metabolism, their level of glycolysis goes down. In these studies separate lines of transgenic mice with increased or decreased glycolysis were used to test if these changes in glucose metabolism altered the development of heart failure induced by pressure overload after transaortic constriction (TAC) surgery. Cardiac glycolysis was targeted by 2 transgenes that alter the level of fructose-2,6-P₂ (F-2,6-P₂), which activates phosphofructokinase. The Mb transgene reduces F-2,6-P₂ and slows glycolysis. The Mk transgene increases F-2,6-P₂ and speeds glycolysis. Mb and Mk transgenic hearts had normal structure and function after sham surgery but they were both much more susceptible to damage from TAC surgery than non-transgenic mice. In both lines of mice TAC produced more fibrosis, more collagen expression, greater hypertrophy, lower fractional shortening, higher lung weight and reduced energy reserves. Mb mice also showed more oxidative stress. These results indicate loss of cardiac flexibility to control glucose metabolism is detrimental to the heart.

Cardiac failure is associated with increased levels of oxidized mitochondrial DNA (mtDNA). It is not known if oxidized mtDNA contributes to cardiac dysfunction. To test if protection of mtDNA can reduce cardiac injury, we produced transgenic mice with cardiomyocyte-specific overexpression of the mitochondrial form of the DNA repair enzyme 8-oxoguanine DNA glycosylase 1 (OGG1). OGG1 transgenic mice demonstrated significantly lower cardiac mitochondrial levels of the DNA guanine oxidation product 7,8-dihydro-8-oxoguanine (8-oxo-dG). This was true under basal conditions, after Doxorubicin administration or after TAC. OGG1 mice were tested for

protection from TAC surgery. Compared to FVB-TAC mice, hearts from OGG1-TAC mice had lower levels of β -MHC mRNA but they did not display significant differences in hypertrophy or function. The principle benefit of OGG1 overexpression was a significant decrease in TAC induced cardiac fibrosis, indicated by reduced Sirius Red staining and by significantly decreased induction of collagen 1 and 3 mRNA expression. These results provide a new model to assess the cardiac effects of mtDNA damage and demonstrate that oxidation of mtDNA contributes to cardiac pathology.

TABLE OF CONTENTS

	PAGE
ACKNOWLEDGMENTS.....	iii
ABSTRACT.....	iv
LIST OF TABLES.....	ix
LIST OF FIGURES.....	x
INTRODUCTION	1
CURRICULUM VITAE.....	112
 CHAPTER	
I. Decreased glycolysis increases susceptibility to cardiac hypertrophy and heart failure	
Introduction.....	5
Methods and Materials.....	6
Results.....	11
Discussion.....	16
II. Increased glycolysis increases susceptibility to cardiac hypertrophy and heart failure	
Introduction.....	40
Methods and Materials.....	41
Results.....	41

Discussion.....	48
III. Cardiac overexpression of mitochondrial 8-oxoguanine DNA glycosylase 1 protects against cardiac fibrosis in heart failure	
Introduction.....	71
Methods and Materials.....	73
Results.....	78
Discussion.....	81
IV. Overview and relevance of dissertation.....	97
REFERENCES.....	101

LIST OF TABLES

TABLE	PAGE
1. Cardiac function measured by echocardiography in FVB and Mb mice 13 weeks after TAC or sham surgery	21
2. Cardiac function measured by echocardiography in FVB and Mk mice 13 weeks later after TAC or sham surgery	52
3. Measurement of heart weight, body weight, tibia length and the ratios of heart weight to body weight and to tibia length in FVB and OGG1 mice 13 weeks after TAC or sham surgery	85
4. Cardiac function measured by echocardiography in FVB and OGG1 mice 13 weeks after TAC or sham surgery	87

LIST OF FIGURES

FIGURE	PAGE
Chapter I	
Figure	
1. The Mb transgene exacerbates TAC induced hypertrophy	23
2. Fibrosis is increased in Mb hearts 13 weeks after TAC	25
3. The ratio of lung weight to tibia length 13 weeks after TAC in FVB and Mb mice	27
4. Hypertrophic biomarkers BNP , ANP , β -MHC and α -MHC mRNAs analyzed by quantitative RT-PCR in FVB and Mb hearts 13 weeks after TAC or sham surgery	29
5. The content of ATP and phosphocreatine (PCr) and the ratio of PCr to ATP in FVB and Mb hearts	31
6. The content F-2,6-P ₂ , lactate and pyruvate in FVB and Mb hearts	33
7. The content of pyridine nucleotides in FVB and Mb hearts.....	35
8. Oxidative stress shown by 4HNE adducts in FVB and Mb hearts	38

Chapter II

Figure

9. The changes of whole heart morphology and heart weight to tibia length ratio in FVB and Mk hearts 13 weeks after TAC	54
10. Fibrosis in FVB and Mk hearts 13 weeks after TAC.....	56
11. The ratio of lung weight to tibia length 13 weeks after TAC in FVB and Mk mice.....	58
12. The content of ATP and phosphocreatine (PCr) and the ratio of PCr to ATP in FVB and Mk hearts after TAC 13 weeks.....	60
13. Hypertrophic biomarkers BNP, ANP, β -MHC and α -MHC mRNAs were analyzed by RT-PCR in FVB and Mk hearts 13 weeks after TAC	62
14. The content of fructose-2,6-bisphosphate (F-2,6-P ₂), glucose-6-phosphate, lactate and pyruvate in FVB and Mk hearts 13 weeks after TAC	64
15. The content of pyridine nucleotides in FVB and Mk hearts 13 weeks after TAC	66
16. Oxidative stress shown by western blot for 4HNE adducts in FVB and Mk hearts 13 weeks after TAC	69

Chapter III

Figure

17. Elevation of OGG1 mRNA, protein and enzyme activity in OGG1 transgenic mice	89
18. Hypertrophic biomarkers β -MHC, α -MHC, ANP and BNP mRNA were analyzed by RT-PCR in OGG1 and FVB hearts 13 weeks after TAC or sham surgery	91
19. Fibrosis in FVB and OGG1 hearts 13 weeks after TAC	93
20. Content of 8-oxo-dG content in mtDNA 13 weeks after TAC	95

INTRODUCTION

Heart failure is the consequence of multiple pathophysiological adaptations and alterations, leading to left ventricular (LV) hypertrophy, dilation and dysfunction. Heart failure can develop as a result of the following models: in the cardiorenal model, heart failure is regarded as a problem of excessive salt and water retention, thus requiring the use of diuretics drugs. In the hemodynamic model, heart failure derives from abnormalities of pumping capacity and excessive peripheral vasoconstriction which can be controlled with the use of inotropic drugs and vasodilators. In the neurohormonal model, heart failure progresses as a result of increased production of biologically active molecules, such as norepinephrine and angiotensin 2, which are capable of exerting deleterious effects on the heart, independent of the hemodynamic status; for this condition, drugs such as beta adrenergic blockers, angiotensin-converting enzyme inhibitors (ACEI) and angiotensin 2 antagonists are used. Although good therapeutic effects have been achieved using beta blockers, ACEI and angiotensin 2 antagonists, the mortality rate from heart failure is still very high. Therefore, new targets for treating heart failure are urgently needed. One emerging target for heart failure therapy involves changes in cardiac metabolism (65).

Under normal conditions, fatty acids provide 70% of the energy for the heart while glucose and lactate provide 30% of the energy (24, 68, 84). Cardiac glucose uptake is driven by a glucose gradient and is dependent on the density of sarcolemmal glucose transporters (Gluts) such as Glut1 and Glut4. Glut1 has a more continuous sarcolemmal location and facilitates basal glucose uptake more so than Glut4. However, Glut4 is the dominant transporter in the adult heart, with a majority of this transporter located in an intracellular pool under basal conditions; upon activation by insulin, Glut4 translocates to the cell membrane to transport glucose (49, 58, 79). Entry of glucose into the cardiomyocyte begins glycolysis. Glycolysis is controlled by a series of enzymes including hexokinase, phosphofructose kinase-1 (PFK-1), phosphofructose kinase-2 (PFK-2), glyceraldehyde 3-phosphate dehydrogenase (GAPDH) and pyruvate kinase (PK) with the end result being the production of pyruvate (16). After glycolysis, pyruvate enters mitochondria for glucose oxidation. The importance of glycolysis is much more than just the metabolism of glucose. ATP derived from glycolysis seems to have a preferential role in maintaining normal conductance of calcium, potassium and sodium ions in the cell membrane (20, 92, 110). Also intermediate products of glycolysis provide the substrates for the synthesis of glycogen, NADPH and other cellular molecules.

The alternate source of cardiac energy, fatty acids (FA), are transported to the heart by way of three FA transport proteins: CD36, FA transport protein (FATP) and FA binding protein plasma membrane (FABPpm) (59). Once the FA enters cardiomyocytes, it is esterified by acyl-CoA synthase (ACS), and the resulting fatty acyl-CoA is

transported into mitochondria for oxidation, or stored as triglycerides (Tg). In normal heart, there is a balance between lipogenesis and lipolysis to control intracellular Tg level (84). If the FA level is much greater than the cellular oxidative capacity, Tg can accumulate and lipotoxicity follows. There is an interaction between glucose metabolism and fatty acid metabolism, called the Randle cycle (34). Increased fatty acid utilization can inhibit glucose oxidation and glycolysis by decreasing pyruvate dehydrogenase complex (PDC) activity and inhibiting PFK-1 activity and glucose uptake. Conversely, hyperglycemia can reduce fatty acid oxidation, probably by increasing the intracellular level of malonyl-CoA to inhibit carnitine palmitoyltransferase I (CPT- I) activity.

Hallmarks for hypertrophied and failing hearts are changes in substrate utilization and energy metabolism. Consistent findings in most forms of heart failure are increased glucose consumption and decreased fatty acid oxidation (38, 101). In contrast, diabetic hearts exhibit the opposite metabolic changes, glucose consumption is decreased and fatty acid oxidation is increased. These diabetic effects on cardiac metabolism are due to insulin resistance in type 2 diabetes and insulin deficiency in type 1 diabetes (22). Notably, diabetes is also an independent risk factor for ultimate development of heart failure (104). Therefore increased or decreased glucose metabolism can play a role in heart failure under different pathological conditions. It is also known that heart failure induced by any cause causes higher levels of oxidative stress (5, 44, 72) in large part due to increased production of mitochondrial reactive oxygen species (ROS). These higher levels of ROS may oxidize mitochondrial DNA (mtDNA) (36). Oxidized mtDNA may further damage mitochondrial function, increase ROS production and worsen heart

failure syndrome in a vicious cycle. Therefore oxidation of mtDNA may play a very important role in the development of heart failure.

Because abnormal cardiac fuel metabolism is closely associated with the progression of heart failure, and because abnormal cardiac metabolism induces more mitochondrial ROS resulting in mtDNA oxidation, we carried out three studies on the pathogenesis of heart failure induced by pressure overload: We tested the hypothesis that reduced glycolysis exacerbates heart failure. We tested the converse hypothesis that increased glycolysis protects from heart failure. Lastly we tested the hypothesis that reduced mtDNA oxidative damage also protect from heart failure. This dissertation is divided into three chapters which correspond to these three hypotheses.

Chapter I: Decreased glycolysis increases susceptibility to cardiac hypertrophy and heart failure

Chapter II: Increased glycolysis increases susceptibility to cardiac hypertrophy and heart failure

Chapter III: Cardiac overexpression of mitochondrial 8-oxoguanine DNA glycosylase 1 protects against cardiac fibrosis in heart failure

Chapter IV: Overview and relevance of dissertation studies

CHAPTER I

DECREASED GLYCOLYSIS INCREASES SUSCEPTIBILITY TO CARDIAC HYPERTROPHY AND HEART FAILURE

INTRODUCTION

Cardiac glucose and fat metabolism are tightly and inversely regulated, as controlled by the Randle cycle (67). Under normal circumstances glucose accounts for only a small portion of cardiac energy supply, but in the failing heart, glucose consumption becomes more important. This has been appreciated for over 40 years since Bishop and Altshud reported (9) that glycolytic metabolism is increased in cardiac hypertrophy and congestive heart failure. However, it is still uncertain whether the elevation of cardiac glucose metabolism is an adaptive response of the failing heart or simply one more example of the prominent reversion to fetal gene expression that occurs during congestive heart failure (CHF) (87).

Most efforts to inhibit cardiac glucose metabolism have utilized knockdown of one of the cardiac glucose transporters (18, 40) but control of glycolysis is actually shared by several reactions (43). One of these reactions is carried out by 6-phosphofructo-1-kinase (PFK1) (33, 70). Unlike glucose transport where there are 2 transporters that can compensate for one another (1), there is only a single PFK1 enzyme.

PFK1 activity is tightly controlled. The most important positive regulator of PFK1 is fructose-2, 6-bisphosphate (F-2, 6-P₂), which is increased several fold in hypertrophied heart (66). We have previously described a transgenic mouse designated Mb (19) which has reduced cardiac levels of F-2,6-P₂ and a subsequent reduction in glycolytic rate.

To test whether prevention of cardiac hypertrophy- induced elevation of F-2,6-P₂ and glycolysis changes the progression of cardiac failure, Mb transgenic mice were subject to pressure overload by transaortic constriction (TAC) for 13 weeks. TAC mimics human aortic stenosis with development of pressure overload induced left ventricular hypertrophy. Heart failure, reductive status and oxidative stress were exacerbated in Mb mice, indicating that up regulation of glycolysis helps protect the heart from chronic pressure overload.

MATERIALS AND METHODS

Animals

Mb transgenic mice (19) and control mice were maintained on the background FVB. Male mice between ages 90–100 days were used for experiments. All animal procedures conformed to the National Institutes of Health *Guide for the Care and Use of Laboratory Animals* (NIH Pub. No. 85-23, Revised 1996) and were approved by the United State Department of Agriculture-certified University of Louisville animal care and use committee.

Transaortic constriction (TAC) surgery

TAC surgery was performed by a modification of a previously published technique (6). Mice were anesthetized with avertin (0.4g/kg), maintained on a 37°C pad and ventilated with 100% oxygen. An incision at the left second intercostal space was made to open the chest. A chest retractor was applied to facilitate the view. The thymus was pulled away and transverse aorta was dissected from surrounding tissues. A 6-0 silk suture was passed around the transverse aorta and tightened against a 26G needle. The needle was immediately removed to provide a lumen with a stenotic aorta. Lungs were inflated and the chest cavity, muscles and skin were closed layer by layer with 6-0 silk sutures. The whole procedure lasted 20-30 min. After surgery, mice were warmed with a heating lamp and received an intraperitoneal injection of 0.5ml of saline at 37°C. For 48 h mice were given subcutaneous injections of buprenorphine, 0.1mg/kg every 12 h. Sham mice were the same as TAC animals except that banding of the transverse aorta was omitted.

Echocardiographic Assessment of Cardiac Function

Transthoracic echocardiography of the left ventricle was performed using a 15-MHz linear array transducer (15L8) interfaced with a Sequoia C512 system (Acuson) as previously described (109). Mice were anesthetized with 2% isoflurane, maintained under anesthesia with 1.25% isoflurane, and examined. Ventricular parameters were measured in M-mode with a sweep speed 200 mm/s. The echocardiograms were captured from short-axis views of the left ventricle (LV) at the midpapillary level. LV percent fractional shortening (LV%FS) was calculated according to the following equation:

$LV\%FS = [(LVEDD - LVESD) / LVEDD] \times 100$. All data were calculated from 10 independent cardiac cycles per experiment.

Quantitative Real Time Polymerase Chain Reaction (RT-PCR)

Cardiac RNA was extracted with Trizol reagent. The total RNA was transcribed to cDNA with Superscript II enzyme and random oligonucleotide primers (Invitrogen). The primers, probes and reaction buffer for RT-PCR were purchased from AB (Applied Biosystem) including α -MHC (alpha myosin heavy chain, Mm01313844_mH), β -MHC (beta myosin heavy chain, Mm00600555_m1), ANP (Atrial natriuretic peptide, Mm01255748_g1), BNP (Brain natriuretic peptide, Mm01255770_g1), procollagen 1 α 1 (Mm01302043_g1), procollagen 3 α 1 (Mm01254476_m1), 18s RNA (Hs99999901_s1) and 2 \times Master buffer. RT-PCR was performed on an AB 7300 thermocycler with 35 cycles, each cycle consisted of 95°C for 15 seconds, 55°C for 15 seconds and 75°C for 30 seconds. 18sRNA was used as endogenous control. Relative abundance of transcripts was determined by the delta-delta CT method.

Histological experiments

Cryostat sections (5 μ m) were fixed in 10% formalin for 15min and washed three times with PBS. The cryostat slides were incubated with a saturated solution of picric acid containing 0.1% Sirius red for staining collagen and 0.1% fast green for staining noncollagen proteins. Staining was performed in the dark for 2 hours. The slides were rinsed with distilled water, dehydrated with alcohol, and mounted with permount. The sections were visualized and photographed by a blinded observer. Interstitial fibrosis was

scored by a blinded observer against reference images using a scale of 1 to 4 based on the severity of fibrosis with scores of 1 for low; 2 for mild; 3 for moderate and 4 for severe.

Western blots

Immunoblotting was performed as previously described (107) with modification. In brief, frozen cardiac tissue was homogenized with lysis buffer containing 50mmol/L Tris-HCl (pH7.5), 5mmol/L EDTA, 10mmol/L EGTA, 1× cocktail protease inhibitor, 1× alkaline phosphatase inhibitor and 1×acid phosphatase inhibitor, 50 ug/ml phenylmethanesulfonyl fluoride and 1.23mg/ml Chaps (3-[(3-Cholamidopropyl) dimethylammonio]-1-propanesulfonate). Extracts were centrifuged at 12000rpm at 4 °C for 15 minutes. The protein concentration was determined by Lowry method (Pierce). Ten ug of the sample proteins was mixed with loading buffer (40mmol/L Tris-HCl, pH 6.8, 1% SDS, 50mmol/L DTT, 7.5% glycerol and 0.003% bromophenol blue) and heated at 95°C for 5 minutes, and subjected to electrophoresis on a gradient gel (4% to 12%, Invitrogen) at 120V. After electrophoresis, the protein was transferred to a PVDF membrane in a transfer buffer (Invitrogen). The PVDF membrane was rinsed briefly in TBS buffer containing 50mM Tris, 137 mM NaCl, pH 7.5 and blocked in buffer (5% milk with 0.5% BSA in TBST buffer (TBS buffer containing 0.1% tween 20) at room temperature for 1 hour. The membrane was then incubated with rabbit anti 4-hydroxy-2-noneal (4HNE) antibody at 1:3000 dilution(Abcam) at 4°C over night, followed by washing three times. The secondary antibody was incubated with the membrane for another one hour at room temperature. Finally the antigen-antibody complexes were

visualized by use of an enhanced chemiluminescence (ECL, GE healthcare) kit. Anti-GAPDH (Abcam) was used for normalization of signals for different samples.

Metabolites measurement

For the assay of lactate, pyruvate, ATP and phosphocreatine, freeze clamped hearts were powdered in liquid nitrogen and weighed. Powdered samples were homogenized in 1M ice cold perchloric acid and centrifuged. Supernatants were neutralized with 2M KHCO_3 . The supernatant from neutralized extracts was used for the estimation of these metabolites by the fluorometric method (55).

For assay of F-2,6- P_2 , freeze clamped heart tissue was homogenized with 10-20 volumes of 50mM NaOH and kept at 80°C for 5min. The extract was cooled and neutralized on ice by adding 1M acetic acid with 20mM HEPES. After centrifugation at 8000g for 10min, the supernatant was collected for F-2,6- P_2 analysis by the PFK-1 activation method (19, 108).

Pyridine nucleotides were measured using a spectrophotometric enzymatic cycling method (8, 116) for both the oxidized and reduced forms of NADP(H) and NAD(H) with modification. Briefly, freeze clamped heart tissue was homogenized with 30 volumes of cold 40mM NaOH containing 0.5mM cysteine buffer for 30 seconds. After centrifuging at 10000rpm for 15min, the supernatant was divided into two parts.

One part was heated at 60°C for 20 min to destroy all NAD(P) for assay of NADH or NADPH, the other part was kept on ice for assay of total NADP(H) or NAD(H). The difference between heated and unheated reactions yields NADP⁺ or NAD⁺ content. For NAD(H) assay, the buffer containing 100mM Tris-HCl, pH 8.0, 2mM PES (phenazine ethosulfate), 0.5mM MTT (3-(4,5-dimethylthiazolyl-2)-2,5-diphenyltetrazolium bromide), 0.2mg/ml ADH (alcohol dehydrogenase) and 600 mM alcohol was used. For assay of NADP(H) buffer containing 100mM Tris-HCl pH 8.0, 5mM EDTA, 2mM PES, 0.5mM MTT, 1.3U/ml G6PDH (glucose-6-phosphate dehydrogenase) and 1.0mM G-6-P (glucose-6-phosphate) was used. The reaction mixtures were kept at room temperature for 15min, then, read by spectrophotometer at 560nm.

Statistical analysis

Statistical comparisons were performed by two-way ANOVA using Sigma Stat software with sham or TAC surgery as one factor and transgenic or non-transgenic as the other factor. The accepted level of significance was 0.05.

RESULTS

Cardiac structural and functional changes after TAC surgery

TAC surgery was performed to assess whether Mb hearts were more sensitive than FVB hearts to pressure overload stress. Thirteen weeks after surgery, both groups of TAC

hearts were significantly enlarged compared to sham hearts (Figure 1). There was no significant difference between Mb-sham and FVB sham hearts but Mb-TAC hearts were significantly larger than FVB-TAC hearts ($p<0.05$). Heart weight to tibia length ratio increased by 49% in FVB mice and by 70% in Mb mice, as a function of TAC versus sham surgery. The results indicate that decreased glycolysis in Mb mice promotes greater hypertrophy in response to pressure overload.

Echocardiography was used to assess the cardiac structural and functional changes (Table 1). Left ventricular end diastolic diameter (LVEDD) and left ventricular end systolic diameter (LVESD) were significantly increased in Mb-TAC and FVB-TAC compared to the corresponding sham hearts. Both LVEDD and LVESD were greater in Mb TAC compared to FVB TAC hearts. Fractional shortening (FS) was reduced by TAC and to a greater extent in Mb-TAC hearts than in FVB-TAC hearts. Thus, in addition to hypertrophy, the Mb transgene worsened the functional response to TAC surgery.

Semiquantative analysis showed that fibrosis was significantly increased 13 weeks after TAC surgery (Figures 2A and B, $p<0.05$). This analysis also showed that interstitial fibrosis staining was greater in Mb-TAC mice compared to FVB-TAC ($p<0.05$). The staining analysis was supported by quantitative RT-PCR assays of cardiac collagen 1 α mRNA expression (Figures 2C). Compared to FVB-TAC mice, expression of collagen 1 α mRNA was 4 fold higher in Mb-TAC mice. Collagen 3 α mRNA also increased, but without significant difference between FVB-TAC and Mb-TAC mice.

An increase in the ratio of lung weight to tibia length is a feature of heart failure. Thirteen weeks after TAC surgery, there was no an increase of this parameter in FVB mice. In contrast, Mb mice showed a significant elevation of lung weight to tibia length ratio (Figure 3), which was 37% higher than the ratio in FVB-TAC mice ($p < 0.05$). This reinforces the impression that the Mb transgene makes the heart more susceptible to pressure overload.

Hypertrophic biomarkers BNP, ANP, β -MHC and α -MHC mRNAs were investigated by quantitative RT-PCR (Figure 4). Expression of each of these biomarkers was significantly changed by TAC surgery. The effect of TAC on BNP, ANP and β -MHC mRNA content was not significantly different in Mb and FVB mice, whereas expression of α -MHC mRNA was significantly lower in Mb-TAC mice compared to FVB-TAC mice.

TAC induced changes in energy reserves, F-2,6-P₂, lactate and pyruvate and in FVB and Mb hearts

In heart failure the ratio of phosphocreatine (PCr) to ATP is a prognostic indicator of survival (69). ATP and PCr were reduced by TAC surgery in both groups of mice (Figure 5). The ratio of PCr to ATP was significantly lower in Mb-TAC hearts compared to FVB-TAC hearts; suggestive of more severely impaired cardiac energy reserves in Mb-TAC mice.

Mb transgenic mice were created to reduce glycolysis by reducing the level of F-2,6-P₂ (19). The reduction in F-2,6-P₂ was confirmed in hearts from Mb-sham mice (Figure 6A). TAC surgery increased cardiac F-2,6-P₂ in both FVB and Mb mice but the F-2,6-P₂ levels in Mb-TAC hearts were still significantly lower than in FVB-TAC hearts. Figures 6B and C show cardiac content for the end products of glycolysis, lactate and pyruvate. In Mb- sham hearts lactate was lower but pyruvate was higher than in FVB-sham hearts. This yields a lower lactate to pyruvate ratio (Figure 6D) which is an indicator of a higher cytosolic reductive status (61) in Mb-sham hearts. After TAC surgery lactate declined significantly in FVB hearts and pyruvate declined significantly in Mb hearts. As a result, after TAC there was no longer a difference in lactate to pyruvate ratio.

The changes of redox status associated with the changes of content of pyridine nucleotides in FVB and Mb hearts

NADH is a reducing agent produced primarily by glycolysis in the cytosol and by the TCA cycle in mitochondria. NADH is a major substrate for ATP production. NAD⁺ is an oxidized form of NADH. The ratio of NADH to NAD also reflects the redox status in cells. Hearts with lower glycolysis in Mb mice contained a lower content of NADH plus NAD⁺ compared to FVB sham (Figure 7A). TAC decreased the total content of NAD(H) (the sum of NAD⁺ and NADH) in both FVB and Mb hearts, and levels were

similar in FVB-TAC and Mb-TAC (Figure 7A). NADH levels were similar in all groups (Figure 7B). NAD^+ content was reduced by TAC surgery and was significantly higher in FVB-sham than in Mb sham (Figure 7C). TAC increased the ratio of NADH/NAD^+ to similar levels in FVB and Mb mice (Figure 7D). Due to the lower NAD^+ content in Mb-sham mice the NADH/NAD^+ ratio was higher in sham treated Mb than in FVB mice.

NADPH usually is regarded as a reducing agent that decreases oxidative stress. NADP^+ is the oxidized form of NADPH. Mb hearts had lower total content of NADP(H) (the sum of NADP^+ and NADPH) compared to FVB hearts after sham or TAC treatment (Figure 7E). TAC reduced NADP(H) in both FVB and Mb mice. TAC decreased NADPH content in Mb and FVB mice but there were no significant differences between Mb and FVB groups. NADP^+ content was significantly reduced by TAC and NADP^+ content was lower in Mb hearts than FVB hearts for both treatment groups. Due to the reduction of both NADPH and NADP^+ , the ratio of NADPH to NADP^+ in FVB TAC did not show a statistical change compared to FVB sham. In contrast, the ratio of NADPH to NADP^+ in Mb TAC increased 3 fold compared to Mb sham and FVB TAC (Figure 7H). This was primarily due to the very low NADP^+ content in Mb TAC hearts (Figure 7G).

The ratio of total NADPH plus NADH to total NADP^+ plus NAD^+ ($\text{NAD(P)H}/\text{NAD(P)}^+$) is an indicator of reductive status and is shown in Figure 7I. Thirteen weeks after TAC, the ratio of NAD(P)H to NAD(P)^+ increased 2-fold in both FVB and Mb hearts. The ratio of $\text{NADP(H)}/\text{NAD(P)}^+$ in Mb TAC was significantly

higher than in FVB TAC. Therefore, TAC increased reductive status and lower glycolysis Mb hearts exhibited a more reduced status after TAC than FVB hearts.

Oxidative stress levels in FVB and Mb after TAC

The protein adduct of 4-hydroxynonenal (4HNE) is a marker of lipid peroxidation and oxidative stress. Western blots of 4HNE adducts (Figure 8) were used to evaluate oxidative stress levels in hearts. TAC increased the level of 4HNE adducts in both FVB and Mb hearts. 4HNE was significantly higher in Mb-TAC than in FVB-TAC hearts.

DISCUSSION

Cardiac structural remodeling and dysfunction after TAC

PFK-1 is one of rate limiting steps that control glycolysis. PFK-1 activity can be controlled by several factors such as citrate, ATP, ADP, H^+ , F-2,6-P₂. The metabolite F-2,6-P₂ is an especially important activator for PFK-1 as shown in previous literature (19, 108). Our laboratory demonstrated in vivo that a decrease of F-2,6-P₂ inhibited glycolysis and an increase of F-2,6-P₂ enhanced glycolysis. TAC treatment increases F-2,6-P₂ content in the heart (66). After TAC, FVB and Mb both exhibited an increase of F-2,6-P₂ content, however, Mb-TAC content was 37% lower than in FVB-TAC, implying that glycolysis in Mb hearts is lower than in FVB hearts after TAC surgery.

Cardiac specific reduction of glycolysis in Mb hearts resulted in more hypertrophy and more severe fibrosis following cardiac insult by pressure over load. Hypertrophic growth in the heart is mediated by growth factor pathways that increase protein synthesis, induce enlargement of cardiomyocytes and promote reorganization of sarcomeres within individual cardiomyocytes. The growth factor pathways for pressure overload (TAC) are stimulated by mechanical stress on the heart. This stress can be transduced by integrins at focal adhesion sites on the cell surface to activate the src tyrosine kinase (50) and the integrin linked kinase (56), which is associated with the cytoskeleton and could rearrange the actin skeleton, leading to hypertrophy. Mechanical stress on cardiomyocytes also induces synthesis and secretion of potent growth factors such as angiotensin 2 (Ang 2) and endothelin-1 (ET-1) to stimulate heart growth (10, 85, 115). Decreased glycolysis in Mb mice might sensitize the heart to the growth factors Ang 2 and ET-1 and/or might predispose the heart to synthesize and secrete more of these growth factors. Elevated Ang2 and ET-1 can also stimulate fibroblasts to produce more fibrosis. In addition, a decrease of glucose utilization would lead to elevation of fatty acid oxidation due to the Randle cycle. Elevated fatty acid oxidation is associated with an increase of oxidative stress. In our mice this possibility is supported by higher 4HNE products in Mb TAC hearts compared to FVB-TAC hearts (Figure 8A and 8B). The increase of oxidative stress may not only stimulate cardiac hypertrophy but also promote fibrosis formation (57, 97, 98). Our data is supported by a cardiac insulin resistance study in which hearts with Glut4 knockout showed cardiac hypertrophy, impaired contractility and increased fibrosis (18, 35, 40) similar to our results. Furthermore the antioxidant tempol prevented cardiac hypertrophy in the Glut4 knockout mice, suggesting that ROS

also might play a role of the hypertrophy response in the Glut4-KO hearts (82) as well as our Mb-TAC hearts.

Mb-TAC hearts also demonstrated more damaged cardiac function than FVB-TAC hearts. This was manifested as a decrease of FS and a higher ratio of lung weight to tibia length, in concert with increased LVEDD and LVESD. A number of membrane transport systems are regulated preferentially by glycolytically generated ATP including the sarcolemmal K_{ATP} channel, voltage-gated Ca^{2+} channels, the Na^+-K^+ pump, the Na^+-H^+ exchanger and the sarcoplasmic reticulum pump (25, 54, 110, 112, 113). Inhibition of glycolysis may have caused diastolic dysfunction (51) due to impairing Excitation-Contraction (E-C) coupling, increasing intracellular Ca^{2+} concentration as well as slowing of Ca^{2+} decay (48). The preferred energy substrate of the hypertrophied myocardium is known to shift from fatty acids to glucose. The utilization of glucose in Mb hearts was lower than in FVB hearts, consequently the glycolysis derived ATP in Mb hearts would be expected to be lower. The importance of glycolysis derived ATP for calcium pumps and channels could be a cause of abnormal calcium homeostasis in Mb hearts. Abnormal calcium homeostasis combined with higher fibrosis (Figure 2) might result in diastolic dysfunction. Diastolic dysfunction was demonstrated by 37% increase of lung weight to tibia length ratio (Figure 3) since impaired diastolic function leads to lung congestion.

Human studies show that failing hearts have a lower PCr/ATP ratio, which is a marker of energy reserve and a predictor of mortality (69). The PCr/ATP ratio was

significantly decreased in Mb-TAC hearts compared to FVB-TAC hearts (Figure 5). Heart failure decreases PCr/ATP ratio, probably due to reducing the content of total adenine nucleotides (90). It is possible this lessened glycolysis might enhance the degradation of adenine nucleotides. The lower PCr/ATP ratio in Mb hearts indicates the energy reserve declined more, thereby contributing to the reduction of systolic contractile force. Furthermore, alpha MHC expression declined more in Mb TAC hearts ($p < 0.05$ vs. FVB TAC, Figure 4) in concert with lower FS and higher LVESD (Table 1). Because alpha MHC has higher ATPase activity and higher filament sliding velocity than beta MHC, down regulation of alpha MHC correlates with systolic dysfunction (83). In addition, increase of alpha MHC expression is protective to the heart (39). Therefore, the lower expression of alpha MHC in Mb-TAC hearts might contribute to the lower contractile force in Mb hearts and probably hastened cardiac failure. All together, lower glycolysis may not only have affected the function of membrane transporters but could have also accelerated the degradation of adenine nucleotides and reduced the expression of alpha MHC, thereby exacerbating impaired heart function under pressure overload.

Changes in pyridine nucleotide content associated with oxidative stress

After TAC, NADPH content declined to the same extent in both FVB and Mb hearts (Figure 7). However, NADP^+ content in Mb TAC decreased more than in FVB-TAC. As a result, the ratio of NADPH to NADP^+ was 3 fold higher than in FVB TAC. If the ratio of both reduced forms, NADH plus NADPH (NAD(P)H) to both oxidized forms, NAD^+ plus NADP^+ (NAD(P)^+) was calculated, the ratio $\text{NAD(P)H}/\text{NAD(P)}^+$ was

statistically higher in Mb TAC than that in FVB TAC hearts, indicating that the Mb-TAC hearts were in a more reduced state. Beyond a certain level, an increased reductive state has been linked to greater cellular oxidative stress (4). This may be because higher NADH and NADPH in mitochondria could cause saturated electron flow in the electron transfer chain (ETC). Some of these electrons can leak out and combine with oxygen, producing superoxide (13). If the mitochondrial ETC was damaged, leakage of electrons could increase and more superoxide would be produced. TAC results in mitochondrial dysfunction in parallel with systolic dysfunction (17). Therefore, the higher ratio of NAD(P)H to NAD(P)⁺ in Mb-TAC hearts could cause stronger oxidative stress from mitochondria. Greater oxidative stress was manifested in Mb-TAC hearts as a higher level of 4HNE adducts (Figure 8). More oxidative stress in the heart is likely to promote damage to multiple components of the cardiomyocyte. Thus the increased reductive state in Mb-TAC hearts may have accelerated the progression of heart failure via increased oxidative stress.

In summary, Mb hearts with reduced glycolysis exhibited greater heart failure after TAC surgery as measured by several parameters including more severe cardiac structural and functional changes, more abnormal energetic status, higher reductive status and higher oxidative stress. These results suggest that decreasing cardiac glycolysis, as occurs in diabetes, can have an important role in the development of diabetes induced heart failure.

Table 1. Cardiac function measured by echocardiography in FVB and Mb mice 13 weeks after TAC or sham surgery

parameter	FVB sham	FVB TAC	Mb sham	Mb TAC
BW (g)	30.4±0.8	30.8±0.8	29.3±0.7	30.6±0.9
LVEDD (mm)	3.81±0.08	4.15±0.05 ^a	3.97±0.08	4.40±0.08 ^{a,b}
LVESD (mm)	2.36±0.10	2.76±0.08 ^a	2.48±0.07	3.17±0.09 ^{a,b}
IVS (D) (mm)	0.91±0.02	1.02±0.03 ^a	0.86±0.03	1.03±0.02 ^a
IVS (S) (mm)	1.18±0.03	1.29±0.03 ^a	1.13±0.02	1.25±0.02 ^a
PWTh (D)(mm)	0.80±0.04	0.89±0.03 ^a	0.74±0.02	0.88±0.03 ^a
PWTh (S)(mm)	1.16±0.04	1.25±0.02 ^a	1.11±0.04	1.25±0.05 ^a
IVS%Th	30.9±2.8	29.3±3.5	33.6±3.6	24.1±2.26
PW%Th	40.7±5.2	40.3±3.8	44.7±1.9	42.0±4.0
IVS/PW	1.16±0.05	1.13±0.03	1.15±0.04	1.15±0.05
%FS	38.6±1.7	33.8±1.1 ^a	37.4±1.3	27.1±1.1 ^{a,b}
HR	487±10	516±11	533±7	525±16

Legend: Data are mean \pm SE. a, $p<0.05$, FVB-sham vs. FVB-TAC or Mb-sham vs. Mb-TAC; b, $p<0.05$, Mb-TAC vs. FVB-TAC by two way ANOVA analysis, $n=8$ for sham groups, $n=12$ for TAC groups. LVEDD, left ventricular end diastolic diameter; LVESD, left ventricular end systolic diameter; IVS(d), interventricular septum thickness at diastole; IVS(s), interventricular septum thickness at systole; PWTh(d), post wall thickness at diastole; PWTh(s), post wall thickness at systole; IVS%Th, interventricular septum % thickening; PW%Th, posterior wall % thickening; IVS/PW, interventricular septum to posterior wall thickness ratio; %FS, percent fractional shortening; HR, heart rates.

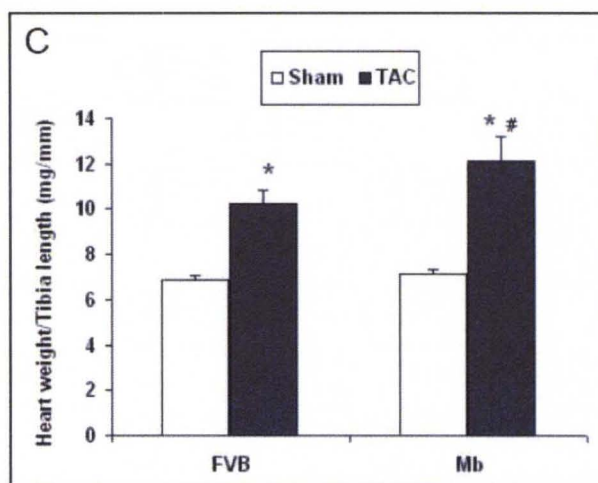
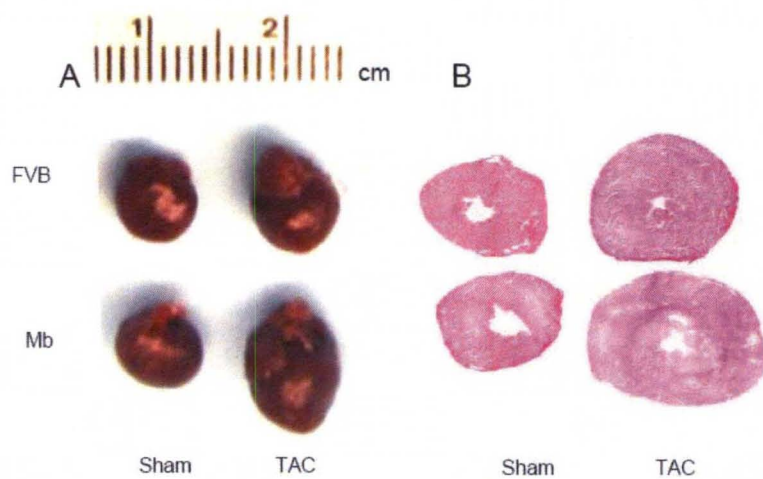


Figure 1. The Mb transgene exacerbates TAC induced hypertrophy. Mice were sacrificed 13 weeks after surgery. Panels A and B show representative whole hearts and transverse cardiac cross-sections, respectively. The graph in panel C shows heart weight to tibia length. Both FVB and Mb TAC hearts were larger than sham hearts. Mb-TAC hearts were larger than FVB-TAC hearts. *, $p < 0.01$, sham vs. TAC; #, $p < 0.05$, Mb-TAC vs. FVB-TAC by two way ANOVA, $n=7$ for FVB-sham, $n=10$ for FVB-TAC, $n=5$ for Mb-sham and $n=7$ for Mb-TAC.

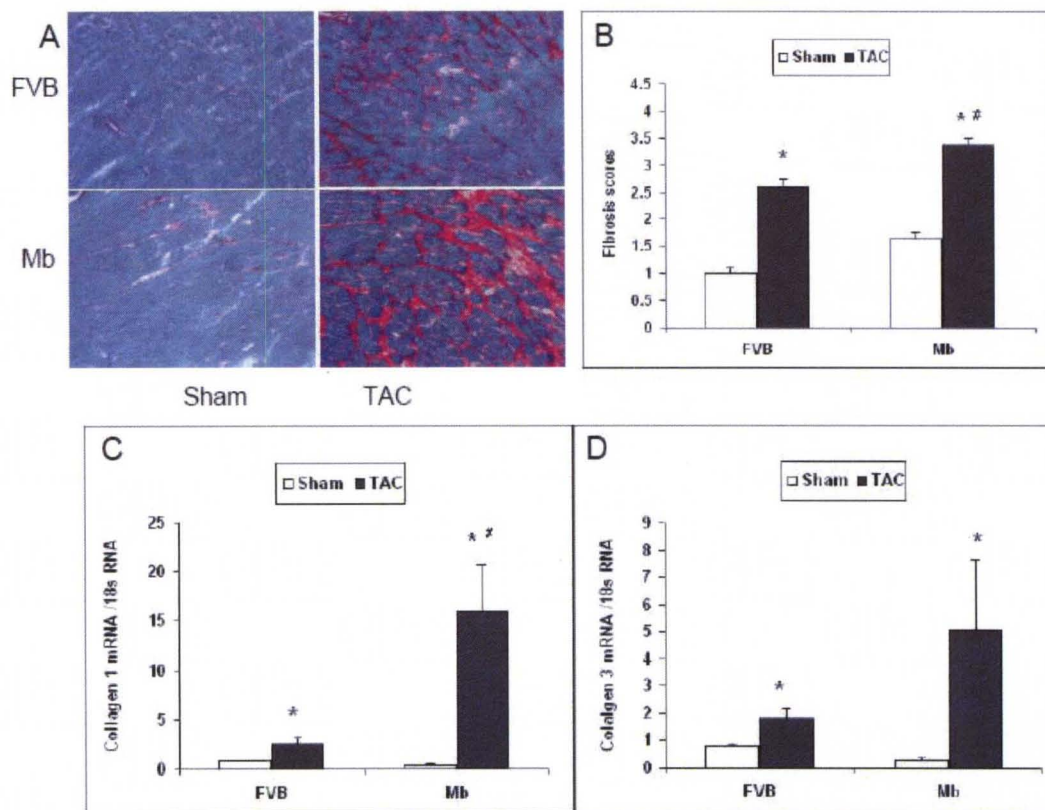


Figure 2. Fibrosis is increased in Mb hearts 13 weeks after TAC. (A) Representative sirius red staining for fibrosis in FVB and Mb hearts. (B) Semi-quantitative scores for fibrosis staining performed as described in Methods by a blind observer. Staining of fibrosis in Mb-TAC hearts was significantly higher than that in FVB-TAC hearts. The expression of collagen 1 α mRNA (panel C) measured by quantitative RT-PCR was significantly higher in Mb-TAC hearts than in FVB-TAC hearts. Expression of collagen 3 α mRNA (panel D) was elevated in TAC hearts but not significantly different in Mb-TAC versus FVB-TAC hearts. #, $P < 0.05$, Mb-TAC vs. FVB-TAC and *, $P < 0.05$, Sham vs. TAC by 2-way ANOVA, $n = 5$ for each group.

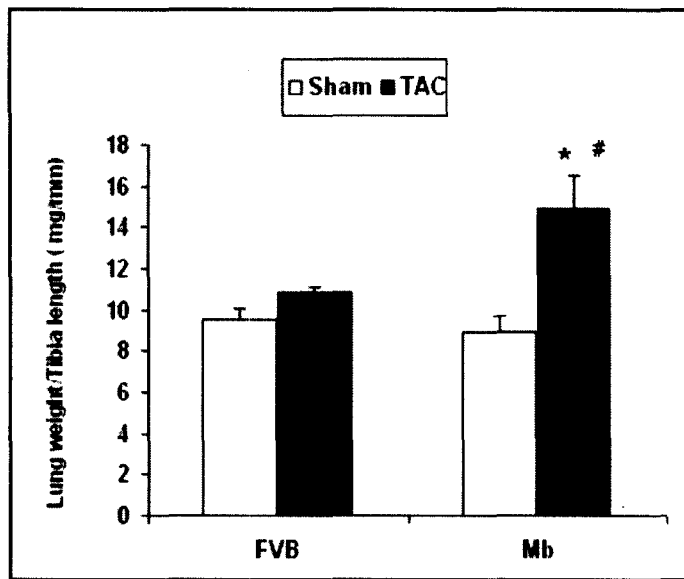


Figure 3. The ratio of lung weight to tibia length 13 weeks after TAC in FVB and Mb mice. TAC significantly increased the ratio of lung weight to tibia length in Mb but not in FVB mice. *, $p < 0.01$, Mb-sham vs. Mb-TAC; #, $p < 0.05$, Mb-TAC vs. FVB-TAC by two way ANOVA analysis, $n=7$ for FVB-sham, $n=10$ for FVB-TAC, $n=5$ for Mb-sham and $n=7$ for Mb-TAC.

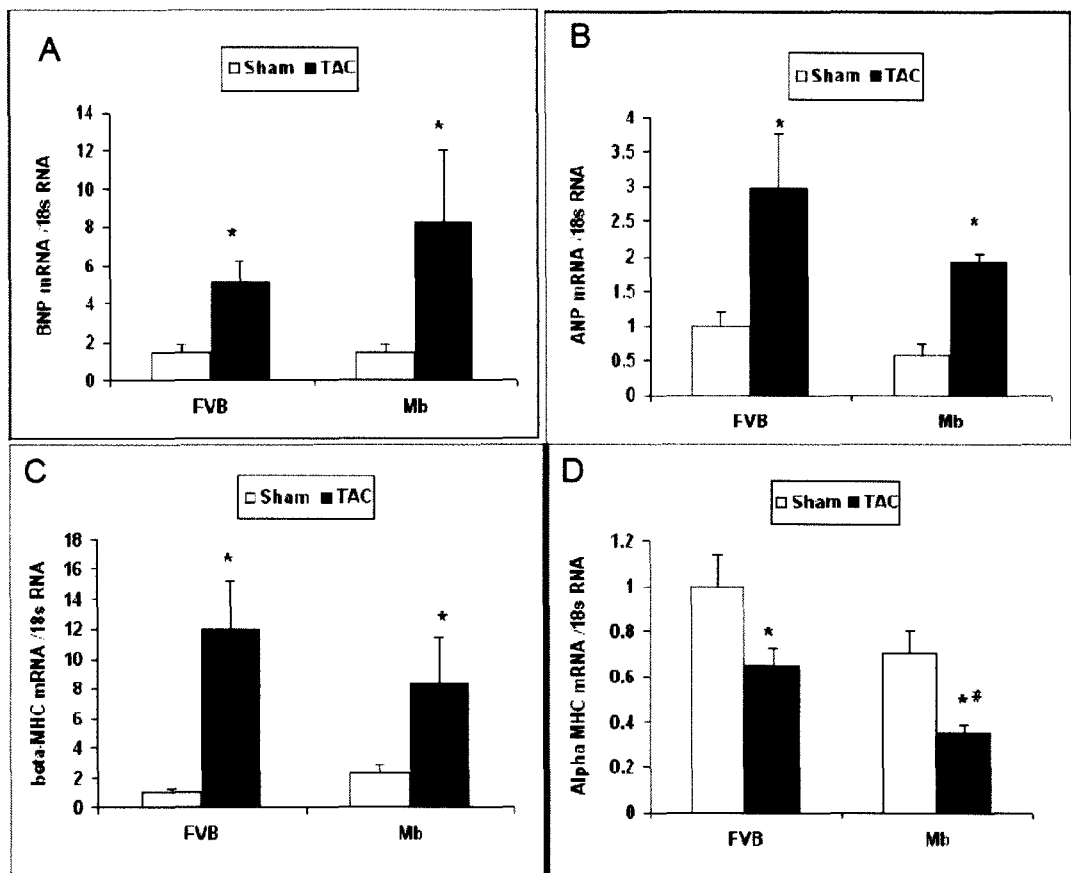


Figure 4. Hypertrophic biomarkers BNP (A), ANP (B), β -MHC (C) and α -MHC (D) mRNAs analyzed by quantitative RT-PCR in FVB and Mb hearts 13 weeks after TAC or sham surgery. Expression of all markers was altered by TAC surgery. Only α -MHC mRNA was significantly different in Mb-TAC compared to FVB-TAC hearts. *, $p < 0.05$, sham vs. TAC; #, $p < 0.05$, Mb TAC vs. FVB TAC by two way ANOVA, $n = 5$ per group.

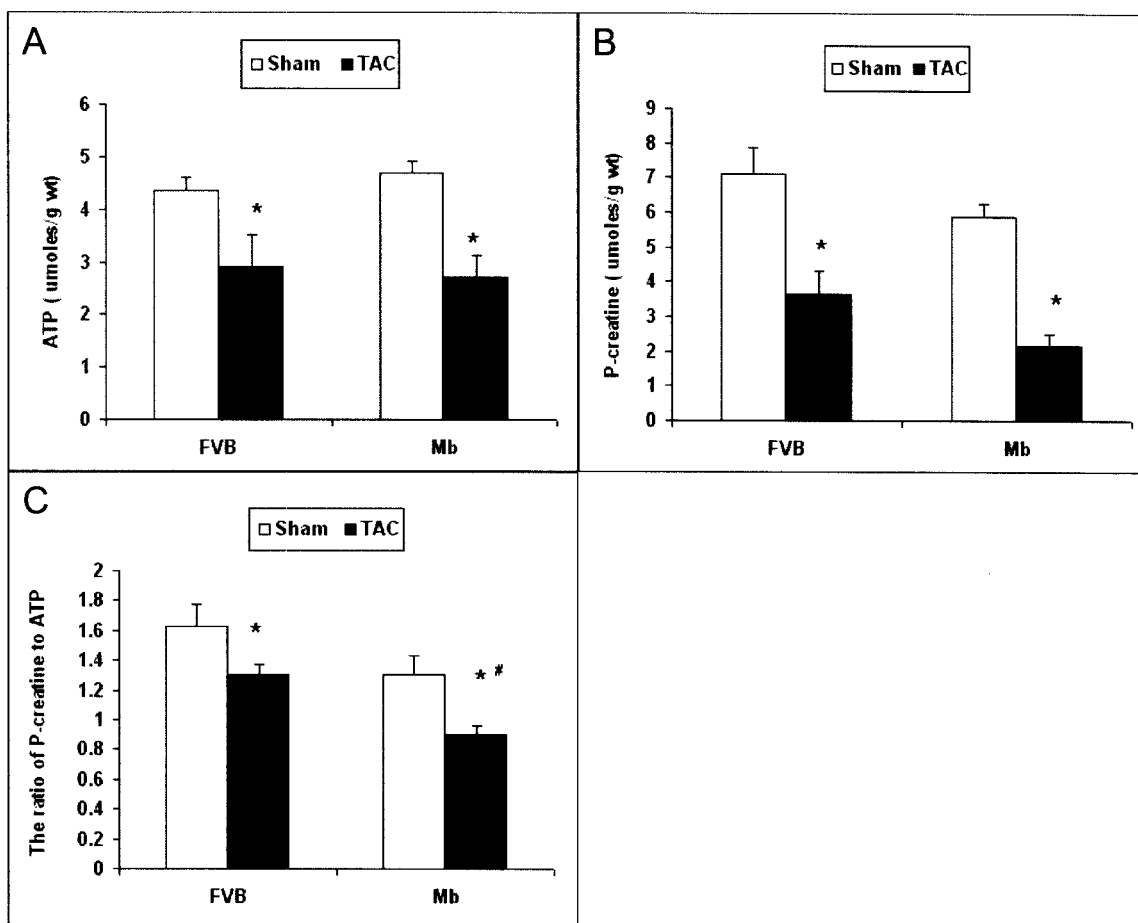


Figure 5. The content of ATP and phosphocreatine (PCr) and the ratio of PCr to ATP in FVB and Mb hearts. (A) and (B) TAC decreased the content of PCr and ATP, however, the differences between FVB and Mb were not significant. (C) TAC decreased the ratio of PCr to ATP in both FVB and Mb mice, moreover, the ratio was lower in Mb-TAC than in FVB-TAC. *, $P < 0.01$, sham vs. TAC; #, $P < 0.05$, FVB TAC vs. Mb TAC by two way ANOVA, $n=8$ for Mb-TAC, $n=5$ for other groups.

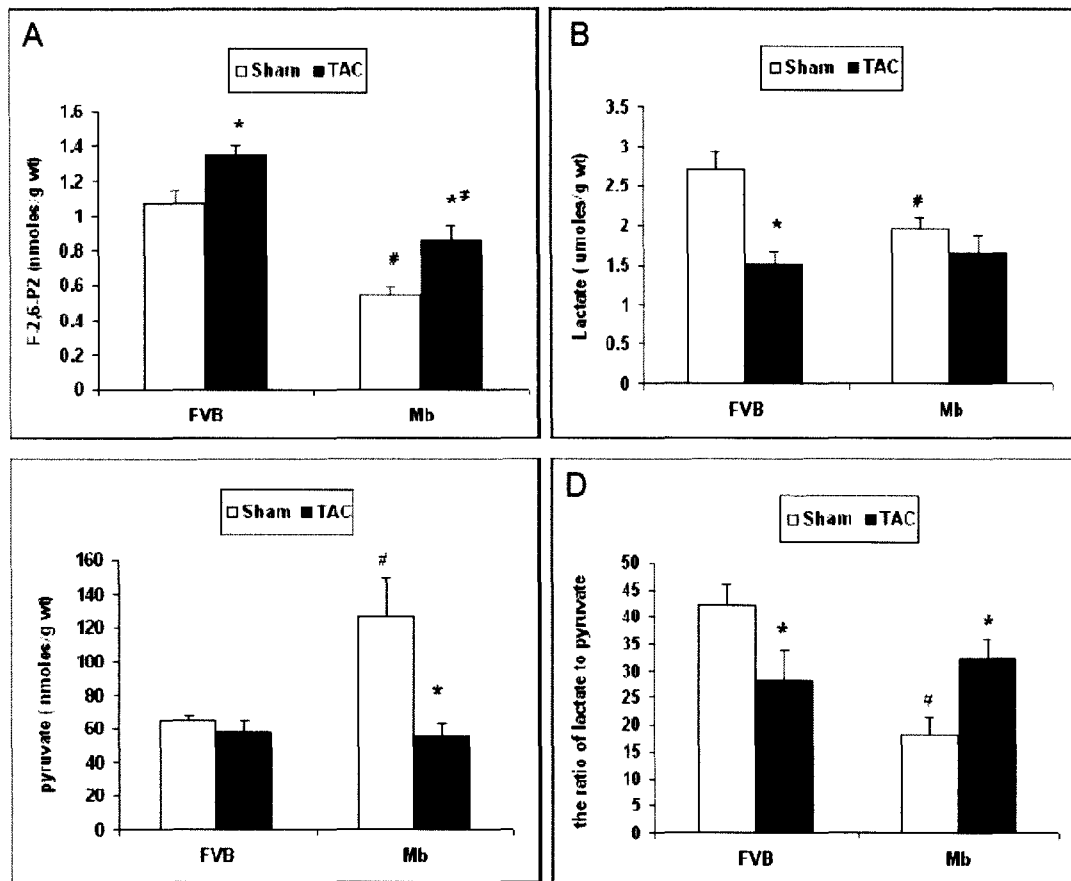


Figure 6. The content F-2,6-P₂, lactate and pyruvate in FVB and Mb hearts. (A)

Cardiac F-2,6-P₂ content was elevated in both groups of TAC mice but always higher in FVB hearts than in Mb hearts. (B) In sham hearts lactate content was lower in Mb mice but in TAC hearts lactate content was similar in Mb and FVB hearts. (C) Mb sham had two fold higher pyruvate content than FVB sham. After TAC, pyruvate content decreased significantly in Mb but not in FVB hearts, as a consequence no significant difference was found in the pyruvate content between FVB-TAC and Mb-TAC. (D) The ratio of lactate to pyruvate in Mb-sham was about one third of that in FVB-sham. After TAC, the ratio of lactate to pyruvate declined in FVB, in contrast, the ratio increased in Mb relative to sham controls respectively. The ratio of lactate to pyruvate in FVB-TAC and Mb TAC was not different. Statistical analysis was done by two way ANOVA, *, $p < 0.05$, sham vs. TAC; #, $p < 0.05$, Mb-sham vs. FVB-sham or Mb-TAC vs. FVB-TAC, $n = 5$ for FVB-sham, Mb-sham and FVB-TAC, $n = 8$ for Mb-TAC.

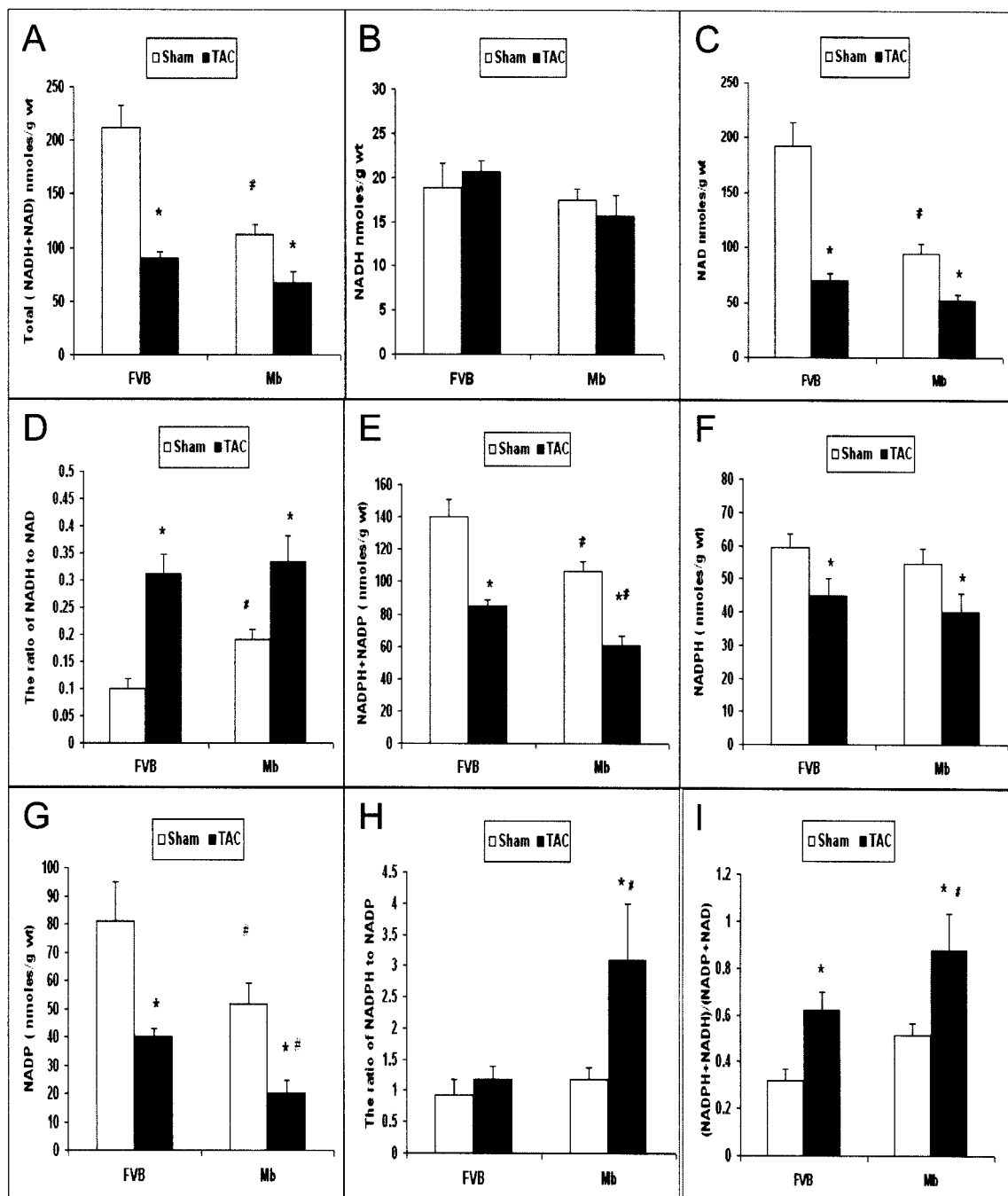


Figure 7. The content of pyridine nucleotides in FVB and Mb hearts. (A) The total of NADH and NAD⁺ content in Mb-sham was reduced to half of that in FVB-sham. After TAC, the total content of NADH plus NAD was decreased significantly in both FVB and Mb hearts, and no significant difference was found between FVB-TAC and Mb-TAC. (B) NADH content was similar in FVB and Mb hearts in all groups. (C) The content of NAD in Mb-sham was significantly lower than in FVB-sham. After TAC, NAD content decreased significantly in both FVB and Mb hearts, whereas no significant difference was found between FVB-TAC and Mb-TAC. (D) The ratio of NADH to NAD was significantly higher in Mb-sham than in FVB sham. After TAC, the ratio in FVB and Mb went up significantly, whereas no significant difference was found when comparing FVB-TAC with Mb-TAC. (E) The total of NADPH and NADP⁺ content decreased by 30% in Mb-sham compared to FVB-sham. TAC reduced the total of NADPH and NADP⁺ content in both FVB and Mb hearts, furthermore, the content of total NADPH plus NADP in Mb-TAC was significantly lower than in FVB-TAC. (F) A significant decrease of NADPH content was observed in FVB and Mb hearts after TAC. The NADPH content was constant in FVB-sham and Mb-sham while no significant difference was found between FVB-TAC and Mb-TAC. (G) NADP⁺ content was lower in Mb-sham compared to FVB-sham. TAC decreased NADP⁺ content in both FVB and Mb hearts and NADP⁺ content in Mb-TAC was significantly lower than in FVB-TAC. (H) TAC increased the ratio of NADPH to NADP⁺ in Mb but not in FVB hearts. Furthermore, the ratio in Mb-TAC was significantly higher than in FVB-TAC. (I) The ratio of reduced pyridine nucleotides, NADPH plus NADH to oxidized nucleotides, NADP⁺ plus NAD⁺ was significantly increased in both FVB and Mb hearts after TAC, and the ratio in Mb-

TAC was significantly greater than in FVB-TAC. *, $p < 0.05$, sham vs. TAC; #, $p < 0.05$, Mb-sham vs. FVB-sham or Mb-TAC vs. FVB-TAC by two way ANOVA analysis, $n = 8$ for Mb-TAC and $n = 5$ for other groups.

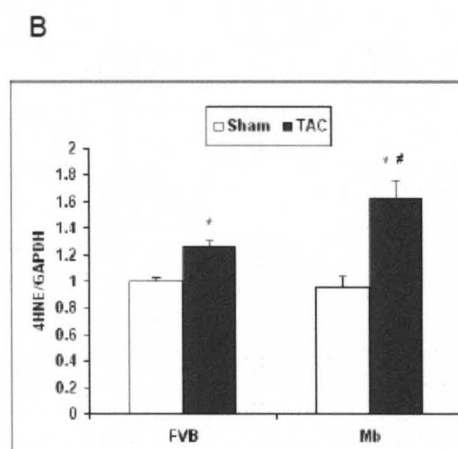
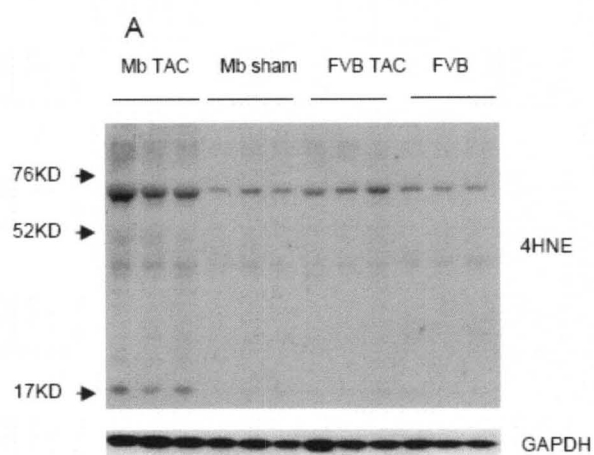


Figure 8. Oxidative stress shown by 4HNE adducts in FVB and Mb hearts. (A)
Representative western blot of 4HNE adducts and GAPDH for loading control. (B)
Statistical results of 4HNE adducts normalized by GAPDH. TAC increased the 4HNE adducts in both FVB and Mb hearts. Mb-TAC exhibited more 4HNE adducts than FVB-TAC. *, $p < 0.05$, sham vs. TAC; #, $p < 0.05$, Mb-TAC vs. FVB-TAC by two way ANOVA analysis, $n=6$ for each group.

CHAPTER II

INCREASED GLYCOLYSIS INCREASES SUSCEPTIBILITY TO CARDIAC HYPERTROPHY AND HEART FAILURE

INTRODUCTION

Heart failure remains the leading cause of mortality in USA. Chronic hemodynamic overload from hypertension, valvular disease or postmyocardial infarction can cause cardiac hypertrophy as a compensatory response. With long term hypertrophy, however, cardiac hypertrophy may evolve into failure, and the underlying mechanism for this transition is poorly understood. A common feature of cardiac hypertrophy and failure is increased glycolysis. This finding is supported by human and animal studies (3, 9, 41, 73, 96, 117). The increase of glycolysis is thought to be adaptive and beneficial (53, 60, 106). The mechanisms for increased glycolysis in hypertrophied heart includes increased glucose uptake by glucose transporters and elevation of F-2,6-P₂ level to enhance PFK-1 activity (66). Tian's group (53) used cardiac specific over expression of the Glut1 transporter to increase glycolysis in the heart. The Glut1 transgene exhibited a protective effect on the heart after aortic banding (53). We used another molecule, fructose-2,6-P₂ (F-2,6-P₂) rather than glucose transporter, to elevate glycolysis in the heart (108). In contrast to the results from Glut1 transgene, our transgenic hearts with high glycolysis induced by elevated levels of F-2,6-P₂ exhibited detrimental effects after banding.

MATERIALS AND METHODS

Animals

The control and Mx mice used were male and kept on the FVB background.

Studies were begun at age 90-100 days and body weight of 26-30g.

Transaortic constriction (TAC) surgery and Echocardiographic Assessment of Cardiac Function

TAC surgery was performed by a modification a previously published (6) as described in chapter I of this dissertation. Transthoracic echocardiography of the left ventricle was performed using a 15-MHz linear array transducer (15L8) interfaced with a Sequoia C512 system (Acuson) as previously described (109) and as detailed in chapter I of this dissertation.

Western blot, Quantitative Real Time Polymerase Chain Reaction (RT-PCR),

Histological experiments, Metabolites measurement and Statistical analysis

The procedures used for these techniques are described in detail in the Methods section of Chapter I

RESULTS

Cardiac structural and functional changes 13 weeks after TAC

TAC was applied for 13 weeks. Both Mk and FVB hearts increased in size (Figure 9A), and hearts from Mk mice appeared larger than those of FVB mice (Figure 9A) after TAC. The change in appearance was also seen in transverse cross-sections of hearts (Figure 9B). The ratio of heart weight to tibia length was used to quantify the morphology change. Heart weight to tibia length ratio increased by 49% in FVB hearts and by 85% in Mk hearts after TAC, and there was a significant difference between FVB-TAC and Mk-TAC (Figure 9C). This result suggests that Mk hearts with increased glycolysis developed more hypertrophy in response to external pressure overload stimuli than normal FVB hearts.

Echocardiography was used to assess cardiac structural and functional changes. Left ventricular end diastolic diameter (LVEDD) and left ventricular end systolic diameter (LVESD) in both FVB and Mk hearts increased significantly after TAC, however, no significant difference was found between FVB TAC and Mk TAC (Table 2). Fractional shortening (FS) in both FVB and Mk decreased significantly after TAC, concomitantly with the changes of LVEDD and LVESD. Furthermore, FS in Mk-TAC declined by 12% compared to FVB-TAC (Table 2) and FS was significantly lower in Mk-TAC hearts. These results indicate that cardiac structure and function in Mk hearts with increased glycolysis were damaged more than in FVB hearts when subject to overload by external pressure.

Fibrosis was examined to evaluate cardiac remodeling due to TAC in Mk and FVB hearts (Figure 10). Figure 10A shows representative pictures of fibrosis staining by

Sirius Red and figure 10B shows semi quantitative analysis of the staining. Fibrosis scores were increased in both FVB and Mk hearts after TAC, whereas the scores in Mk-TAC were statistically higher than in FVB-TAC. The expression of collagen 1 and collagen 3 mRNA level confirmed the results of fibrosis staining (Figure 10C and 10D). The mRNA level of collagen 1 and collagen 3 were elevated significantly ($p<0.01$) in Mk and FVB after TAC and the expression of collagen 1 mRNA and 3 mRNA level was higher ($p<0.05$) in Mk-TAC compared to FVB-TAC hearts (Figure 10C and 10D). The greater fibrosis in Mk hearts indicates that increased glycolysis might promote more severe cardiac remodeling.

Lung weight to tibia length ratio is a good indicator of heart failure. This parameter was also measured to evaluate heart function. Thirteen weeks after TAC, FVB mice did not exhibit any significant change in the lung weight to tibia length ratio. In contrast, Mk mice showed a significant elevation of the lung weight to tibia length ratio (Figure 11). Furthermore, the ratio in Mk-TAC increased by 61% ($p<0.05$) compared to FVB-TAC. This implies that hearts with increased glycolysis reached more severe heart failure than hearts with normal glycoysis in response to external pressure overload. Therefore, the hearts with increased glycolysis in Mk mice seems to be more vulnerable to the pressure overload stimulus, exhibiting a greater hypertrophy response and a more severe decrease of cardiac function.

Changes of energetic status in FVB and Mk hearts after TAC and sham surgery

Due to the decrease of systolic function after TAC, the supply of high energy compounds, ATP, and phosphocreatine (PCr) and the ratio of PCr to ATP were measured. The ratio of PCr to ATP is the most widely used indicator of cardiac muscle reserve. After TAC, ATP content was significantly decreased in FVB, while TAC reduced the ATP content in Mk mice but without reaching significance (Figure 12A). In addition, TAC decreased the level of PCr and the ratio of PCr to ATP ($P<0.05$) in both FVB and Mk mice (Figure 12B and 12C). Regarding the levels of ATP and PCr, there were no significant difference between FVB-sham and Mk-sham and between FVB-TAC and Mk-TAC (Figure 12A and 12B), whereas, the ratio of PCr to ATP was a significant decreased by 28% in Mk-TAC compared to FVB-TAC hearts (Figure 12C). Thus, TAC decreased energy reserve in hearts, and hearts with higher glycolysis in Mk mice potentiated the reduction of energy reserve. This reduction of energy reserve might contribute to systolic dysfunction in Mk mice.

Hypertrophic biomarkers of expression of BNP, ANP, β -MHC and α -MHC mRNA

Mk mice exhibited more hypertrophy, manifested as an elevated ratio of heart weight to tibia length after TAC. The hypertrophic biomarkers BNP, ANP, β -MHC and α -MHC mRNA were investigated by RT-PCR in both Mk and FVB mice. The expression of BNP, ANP and β -MHC mRNA level increased significantly in both Mk and FVB mice after TAC, whereas no statistical differences were found between FVB-TAC and Mk-TAC hearts, and between FVB-sham and Mk-sham hearts (Figure 13A, 13B and 13C). The expression level of α -MHC mRNA decreased significantly in both FVB and Mk

mice after TAC, however, without a significant changes in Mk-TAC compared to FVB-TAC (Figure 13D).

The levels of fructose-2,6-P₂, glucose-6-phosphate, lactate and pyruvate metabolites after TAC and sham surgery

The level of fructose-2,6-P₂ (F-2,6-P₂) was manipulated to control glycolysis in Mk mice, in which the content of F-2,6-P₂ was 7 fold higher than that in FVB wild type (1.06±0.08 vs.7.58±0.72 nmoles/g wt in FVB-sham and Mk sham, respectively, p<0.01, Figure 14A). Thirteen weeks after TAC the content of F-2,6-P₂ was increased in both FVB and Mk hearts and the F-2,6-P₂ level in Mk-TAC (9.69±0.37 nmoles/g wt) was still higher than that in FVB-TAC hearts (1.34±0.06 nmoles/g wt, p<0.05, Figure 14A), suggesting that glycolysis continued to be higher in Mk hearts. Glucose-6-phosphate (G-6-P) levels were lower in Mk-sham hearts than in FVB-sham hearts (p<0.05). TAC further decreased the content of G-6-P in both FVB and Mk hearts, with a significantly lower G-6-P level in Mk-TAC than in FVB-TAC hearts (Figure 14B). Since G-6-P is upstream of PFK1 the lower levels of G-6-P in Mk hearts is consistent with more active PFK1 due to higher levels of F-2,6-P₂ in Mk hearts both before and after TAC. Lactate is a product of glycolysis, and therefore has been used as an indirect indicator of glycolysis. As expected, lactate in Mk-sham hearts (4.56±0.52 umoles/g wt) increased by 68% compared to FVB-sham hearts (2.71±0.24 umoles/g wt, Figure 14C), consistent with the elevation of F-2,6-P₂ in Mk mice (Figure 14A). TAC decreased lactate in FVB and Mk mice, perhaps because of higher glucose oxidation rates following TAC. After TAC,

lactate in Mk hearts was two-fold higher than in FVB hearts (Figure 14C). Pyruvate content in Mk hearts was also higher than in FVB hearts, either with or without TAC surgery (Figure 14D). The higher content of lactate and pyruvate, which are both downstream products of the key glycolytic enzyme PFK1, are consistent with elevated glycolytic rate in Mk hearts before and after TAC surgery.

The changes of redox status associated with the changes of content of pyridine nucleotides in FVB and Mk hearts

NADH is produced primarily by glycolysis in the cytosol and the TCA cycle in mitochondria. NADH is a major substrate for ATP production. NAD^+ is the oxidized form of NADH. The ratio of NADH to NAD^+ reflects the redox status in cells. Mk hearts exhibited a lower total content of NADH plus NAD^+ compared to FVB-sham hearts (Figure 15A). TAC decreased the total content of NAD(H) (NADH plus NAD^+) in FVB hearts but not in Mk hearts (Figure 15A). NADH content was lower in Mk-sham than FVB-sham hearts (Figure 15B). TAC did not have any effects on NADH level in FVB mice (Figure 15B), but unexpectedly TAC increased NADH levels in Mk hearts (Figure 15B). Similar to NADH, NAD^+ levels were also lower in Mk-sham than in FVB-sham (Figure 15C). TAC decreased the NAD^+ level in FVB hearts and had no significant effect on NAD^+ content in Mk hearts (Figure 15C). Consequently, NAD^+ levels in Mk-TAC and FVB-TAC hearts were similar (Figure 15C). The ratio of NADH to NAD^+ was significantly increased in both FVB and Mk hearts by TAC, but there were no significant

differences in this ratio between Mk and FVB hearts for either sham or TAC groups (Figure 15D). Therefore, in FVB hearts the reason for the increased ratio of NADH to NAD^+ after TAC was the decline in NAD^+ content. Conversely, in Mk hearts the ratio of NADH to NAD^+ increased after TAC because NADH content went up.

NADPH is produced primarily by the cytosolic pentose phosphate pathway and is important for antioxidant protection. NADP^+ is the oxidized form of NADPH. Mk-sham hearts exhibited a lower total content of NADP(H) compared to FVB-sham hearts (Figure 15E). After TAC, the total content of NADP(H) decreased significantly in FVB but not in Mk hearts (Figure 15E). Mk-sham hearts exhibited a lower level of NADPH compared to FVB-sham hearts (Figure 15F). TAC decreased the level of NADPH in FVB mice (Figure 15F). Unexpectedly, TAC increased NADPH content in Mk-TAC hearts to a significantly higher level than in Mk-sham or FVB-TAC hearts (Figure 15F). Mk-sham and Mk-TAC hearts exhibited a significantly lower level of NADP^+ than the corresponding FVB groups (Figure 15G). TAC lowered NADP^+ levels in Mk and FVB hearts. Since TAC both increased NADPH and reduced NADP^+ in Mk hearts the ratio of NADPH to NADP^+ was very high in Mk-TAC hearts (Figure 15H) and this was significantly higher than any other group.

The combined reductive pyridine nucleotide status, an indicator of overall cellular reductive status can be calculated as the ratio of total NADPH plus NADH to total NADP^+ plus NAD^+ (NAD(P)H/NAD(P)^+) as shown in Figure 15I. Thirteen weeks after TAC surgery, the ratio of NAD(P)H to NAD(P)^+ was elevated significantly in both

FVB and Mk hearts. The ratio of NADP(H)/NAD(P)⁺ in Mk-TAC was statistically higher than in FVB-TAC.

Oxidative stress marker in FVB and Mk hearts after TAC surgery

The protein adduct of 4-hydroxynonenal (4HNE) is a marker of lipid peroxidation and oxidative stress. 4HNE western blots (Figure 16) were used to evaluate oxidative stress levels in hearts. TAC increased the level of 4HNE adducts in both FVB and Mk mice, without a significant difference between Mk-TAC and FVB-TAC groups.

DISCUSSION

PFK-1 is one of rate limiting steps that control glycolysis. PFK-1 activity can be controlled by several factors such as citrate, ATP, ADP, H⁺, F-2,6-P₂. In our Mk transgenic mice, F-2,6-P₂ was increased several fold before and after TAC, which activates PFK-1, increases glycolysis measured in perfused hearts by 50% (108) and decreases Glucose-6-P (G-6-P) levels. The decrease in G-6-P content is consistent with the concept that increased PFK-1 activity will reduce the level of PFK1 substrates. The reduction of NADPH level in Mk-sham hearts (Figure 15F) may have been due to the lower level of G-6-P in Mk hearts, since G-6-P is the first substrate of the pentose phosphate pathway, which produces NADPH. Unexpectedly NADPH levels were much higher in Mk-TAC hearts than in FVB-TAC or Mk-sham hearts (Figure 15F). Since NADPH has antioxidant value, this suggests that Mk-TAC could be protected from

oxidative stress. However, Mk TAC hearts demonstrated the same level of 4HNE adducts as FVB TAC hearts (Figure 16), suggesting that oxidative stress might not be the reason for greater deterioration of cardiac function in Mk-TAC compared to FVB-TAC hearts.

The paradoxical finding of lower G-6-P content, concurrently with higher NADPH levels in Mk-TAC hearts suggests that the higher NADPH was probably produced from pyridine nucleotide transhydrogenases in mitochondria rather than from the pentose pathway in the cytosol. NADH can reduce NADP^+ to NADPH by mitochondrial transhydrogenases (31, 94), which can account for 45% of the total NADPH supply. The remainder is provided by NADP^+ dependent isocitrate dehydrogenase and the mitochondrial NADP^+ dependent malic enzyme (86, 89, 105). NAD^+ cannot diffuse between cytosol and mitochondria (111). Thus, a question should be raised about the balance of NADPH in cytosol versus mitochondria. Therefore, the change of cytosolic and mitochondrial NADPH level is worth investigating in Mk-TAC hearts, to possibly explain the lower content of G-6-P concurrent with high levels of NADPH and the lack of protection from oxidative stress.

Comparison of cardiac energy reserves in Mk mice to another transgenic model of increased glycolysis

A transgenic mouse with cardiac specific overexpression of the Glut1 transporter produced 40 fold higher glucose uptake, 5 fold higher cardiac glycogen and markedly increased lactate (53). This indicated that Glut1 overexpression increased glycolysis and

caused increased cardiac content of glycolytic metabolites . Although glycolysis was increased in both Mk and Glut1 transgenic hearts, the different levels of PFK activity and glucose uptake might have different effects on the heart. After aortic banding, the Glut1 transgene exhibited a protective effect with preserved energy reserve e.g. higher PCr/ATP ratio (53). In contrast, the Mk transgene produced a detrimental effect after TAC with lower energy reserve e.g. lower PCr/ATP ratio. This suggests that increased glycolysis initiated by the glucose transporter or initiated by elevation of PFK-1 activity have opposite effects on energy reserve in the stressed heart. Human studies showed that failing hearts have a lower PCr/ATP ratio, which predicted mortality(69). Animal studies demonstrated that TAC decreased the PCr/ATP ratio probably due to reduction of total adenine nucleotide content (90). Therefore, increased glycolysis by increased rate of glucose uptake via glucose transporter higher than PFK-1 activity might preserve the TAN (total adenine nucleotide) content, whereas increase of glycolysis by elevation of PFK activity higher than the rate of glucose uptake via glucose transporter might potentiate the reduction of TAN after banding.

Mk exacerbation of TAC injury to the heart

Cardiac specific increased glycolysis by elevation of F-2,6-P₂ level in Mk hearts produced more hypertrophy, more severe fibrosis, lower energy reserves and more impaired cardiac function following pressure over load. The mechanistic basis for the negative effects of Mk are not yet certain and will require a further understanding of the basis of cardiac hypertrophy and heart failure. The purpose of cardiac hypertrophy is to relieve stress on the ventricular wall. The mechanical stress produced by TAC can cause

integrins to activate src tyrosine kinase (50) and the integrin linked kinase (56), leading to rearrangement of actin skeleton, while mechanical stress could also induce synthesis and secretion of potent growth factors such as angiotensin 2 (Ang 2) and endothelin-1 (ET-1) to stimuli heart growth (10, 85, 115). Therefore, it is possible that increased glycolysis by elevation of the F-2,6-P₂ level in Mk hearts might amplify the src tyrosine kinase or integrin linked kinase signals or change the behavior of Mk cardiomyocytes to secrete more Ang2 or ET-1 under stress conditions, which could also impact fibroblasts to produce more fibrosis.

Mk transgene summary

In summary, Mk hearts after TAC exhibited more severe structural and functional changes than FVB hearts. Since a publication reported that elevation of glycolysis by the Glut1 transporter protected hearts from pressure overload, it appears that the mechanism of glycolysis elevation is critical. Our current results suggest that therapeutic interventions in heart failure aimed at altering metabolism to protect the heart would be better by focusing on increasing glucose uptake, rather than increasing PFK1 activity. Our results also suggest that the increase F-2,6-P₂ content that occurs in failing hearts is more likely to be detrimental rather than a beneficial, adaptive response.

Table 2. Cardiac function measured by echocardiography in FVB and Mk mice 13 weeks later after TAC or sham surgery

parameter	FVB sham	FVB TAC	Mk sham	Mk TAC
BW (g)	30.4±0.8	30.8±0.8	30.8±1.3	29.4±0.9
LVEDD (mm)	3.81±0.08	4.15±0.05 ^a	4.13±0.06 ^c	4.18±0.06
LVESD (mm)	2.36±0.10	2.76±0.08 ^a	2.46±0.07	2.95±0.07 ^a
IVS (d) (mm)	0.91±0.02	1.02±0.03 ^a	0.94±0.02	1.02±0.03 ^a
IVS (s) (mm)	1.18±0.03	1.29±0.03	1.3±0.04	1.28±0.03
PWTh (d) (mm)	0.80±0.04	0.89±0.03 ^a	0.79±0.02	0.92±0.03 ^a
PWTh (s) (mm)	1.16±0.04	1.25±0.02 ^a	1.20±0.03	1.28±0.03 ^a
IVS%Th	30.9±2.8	29.3±3.5	38.2±4.9	26.9±4.7
PW%Th	40.7±5.2	40.3±3.8	55.6±2.8	40.7±3.1
IVS/PW	1.16±0.05	1.13±0.03	1.22±0.04	1.12±0.04
%FS	38.6±1.7	33.8±1.1 ^a	40.4±1.1	29.6±1.3 ^{a,b}
HR	487±10	516±11	475±15	525±12

Legend: Data are mean \pm SE. a, $p<0.05$, FVB-sham vs. FVB-TAC or Mk-sham vs. Mk-TAC; b, $p<0.05$, Mk-TAC vs. FVB-TAC; c, $p<0.05$, Mk-sham vs. FVB-sham by two way ANOVA analysis, n=8 for sham groups, n=12 for TAC groups. LVEDD, left ventricular end diastolic diameter; LVESD, left ventricular end systolic diameter; IVS(d), interventricular septum thickness at diastole; IVS(s), interventricular septum thickness at systole; PWTh(d), post wall thickness at diastole; PWTh(s), post wall thickness at systole; IVS%Th, interventricular septum % thickening; PW%Th, posterior wall % thickening; IVS/PW, interventricular septum to posterior wall thickness ratio; %FS, percent fractional shortening; EF, ejection fraction; HR, heart rates.

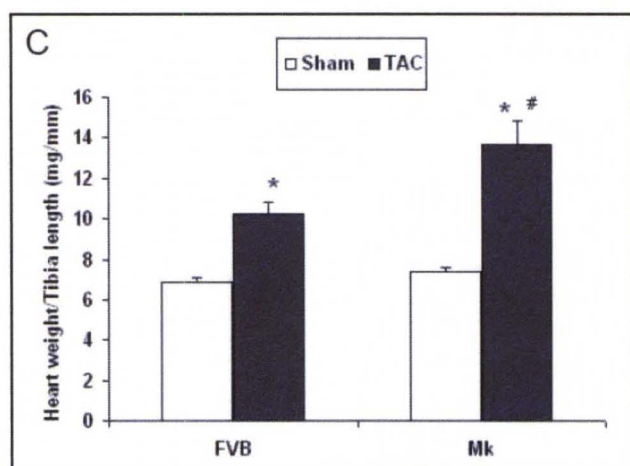
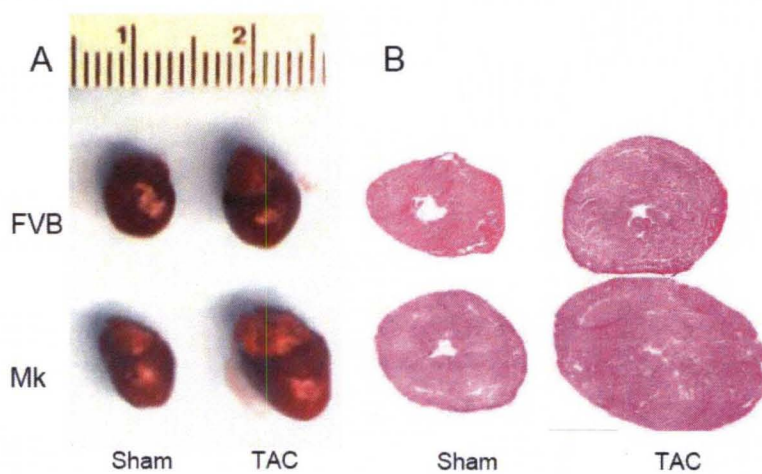


Figure 9. The changes of whole heart morphology and heart weight to tibia length ratio in FVB and Mk hearts 13 weeks after TAC. (A) Representative morphology of whole hearts 13 weeks after TAC. (B) Representative transverse cross-sections of hearts after TAC, confirming the hypertrophy of whole hearts in (A). (C) The ratio of heart weight to tibia length after TAC. Both FVB and Mk had significantly higher heart weight to tibia length ratio after TAC, moreover, the ratio in Mk-TAC was significantly higher than that in FVB-TAC. *, $p < 0.01$, sham vs. TAC; #, $p < 0.05$, Mk-TAC vs. FVB-TAC by two way ANOVA analysis, $n=7$ for FVB-sham, $n=10$ for FVB-TAC, $n=6$ for Mk-sham and $n=9$ for Mk-TAC.

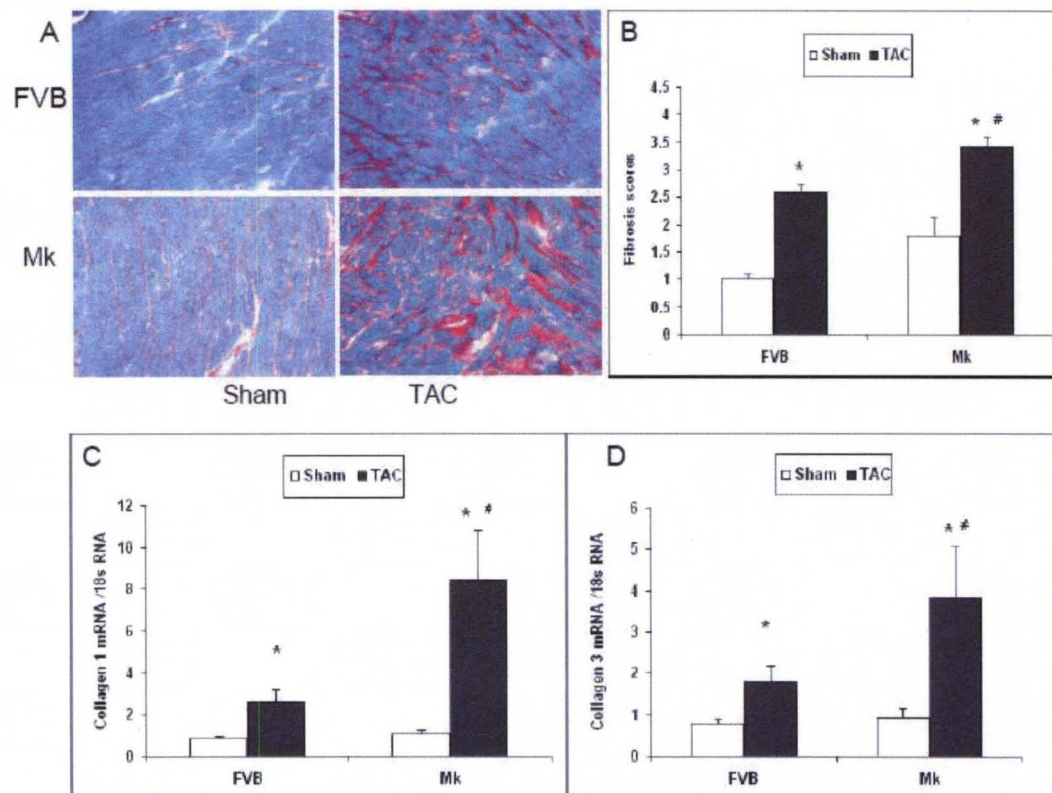


Figure 10. Fibrosis in FVB and Mk hearts 13 weeks after TAC. (A) Representative staining for fibrosis in FVB and Mk hearts after sham and TAC surgery. (B) Semi-quantitative analysis of fibrosis measured by staining with Sirius Red and scored by estimating fibrosis: staining graded as 1 for low, 2 for mild, 3 for moderate and 4 for severe. The staining of fibrosis in Mk and FVB was increased significantly after TAC, moreover, the fibrosis staining scores in Mk-TAC was significantly higher than the scores in FVB-TAC. (C) and (D) The expression of collagen 1 and collagen 3 mRNA was analyzed by quantitative RT-PCR. The expression of collagen 1 and 3 mRNA was increased significantly in both FVB and Mk mice after TAC, furthermore, the expression of collagen 1 mRNA and collagen 3 mRNA was significantly higher in Mk-TAC comparing with FVB-TAC, confirming the fibrosis staining in (A) and (B). *, $p < 0.05$, sham vs. TAC; #, $P < 0.05$, Mk-TAC vs. FVB-TAC by two way ANOVA analysis, $n = 5$ for each group.

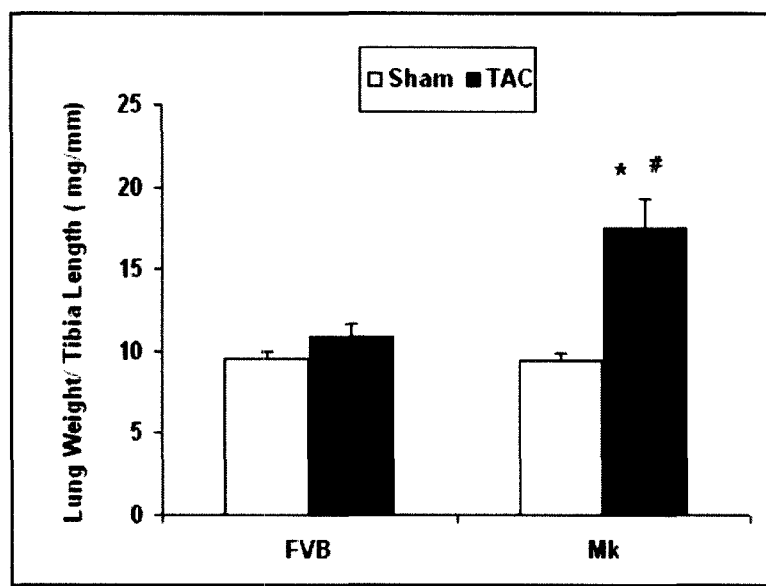


Figure 11. The ratio of lung weight to tibia length 13 weeks after TAC in FVB and Mk mice. TAC significantly increased the ratio of lung weight to tibia length in Mk not in FVB mice. Further analysis revealed that Mk-TAC had significantly higher ratio of lung weight to tibia length than FVB-TAC. *, $p < 0.01$, Mk-sham vs. Mk-TAC; #, $p < 0.05$, Mk-TAC vs. FVB-TAC by two way ANOVA analysis, $n=7$ for FVB-sham, $n=10$ for FVB-TAC, $n=8$ for Mk-sham and $n=12$ for Mk-TAC.

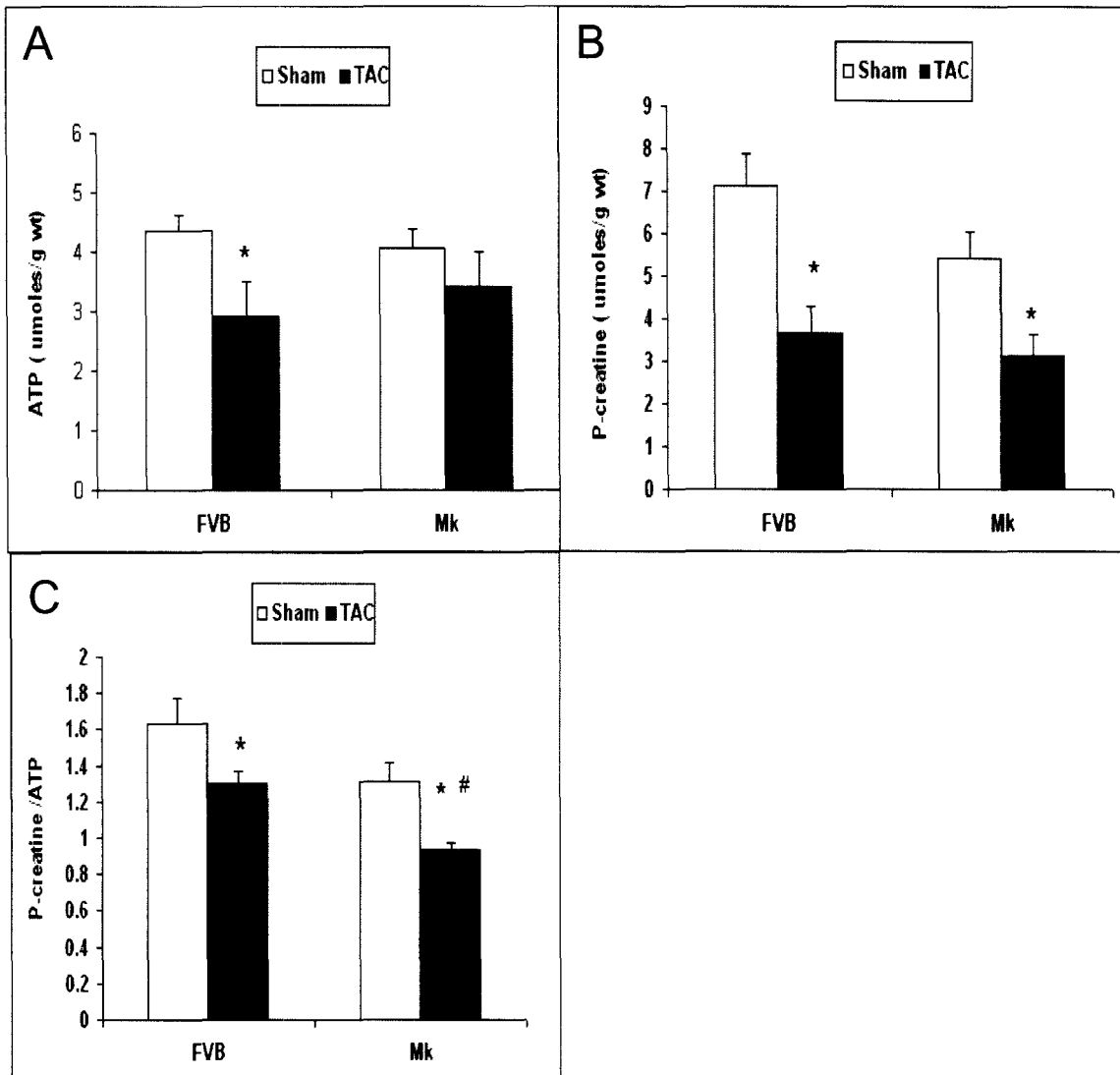


Figure 12. The content of ATP and phosphocreatine (PCr) and the ratio of PCr to ATP in FVB and Mk hearts after TAC 13 weeks. (A) TAC significantly decreased the level of ATP in FVB and Mk hearts to a similar level. No significant difference was found between FVB-sham and Mk-sham and in between FVB-TAC and Mk-TAC. (B) TAC decreased the content of PCr in both FVB and Mk, however, no significant difference was found between FVB-sham and Mk-sham and between FVB-TAC and Mk-TAC. (C) TAC decreased the ratio of PCr to ATP in both FVB and Mk mice, furthermore, a significant decrease of the ratio was found in Mk-TAC compared to FVB-TAC. *, $p < 0.01$, sham vs. TAC; #, $p < 0.05$, FVB-TAC vs. Mk-TAC by two way ANOVA analysis, $n=5$ for each group.

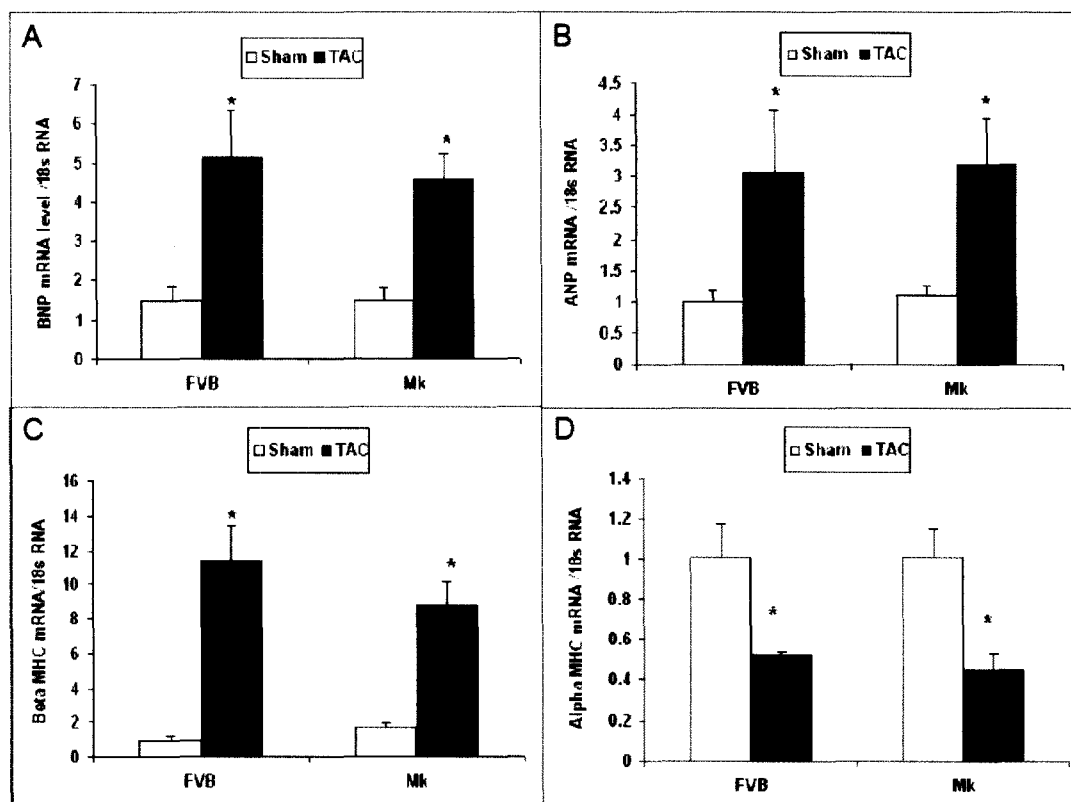


Figure 13. Hypertrophic biomarkers BNP, ANP, β -MHC and α -MHC mRNAs were analyzed by RT-PCR in FVB and Mk hearts 13 weeks after TAC. (A), (B) and (C)

The expression of ANP, BNP and β -MHC was increased significantly in both Mk and FVB mice after TAC, however, no significant differences were found between FVB-TAC and Mk-TAC. (D) The expression of α -MHC mRNA decreased significantly in both FVB and Mk hearts after TAC, without significant difference between Mk-TAC and FVB-TAC. *, $p < 0.05$, sham vs. TAC by two way ANOVA analysis, $n = 5$ for each group.

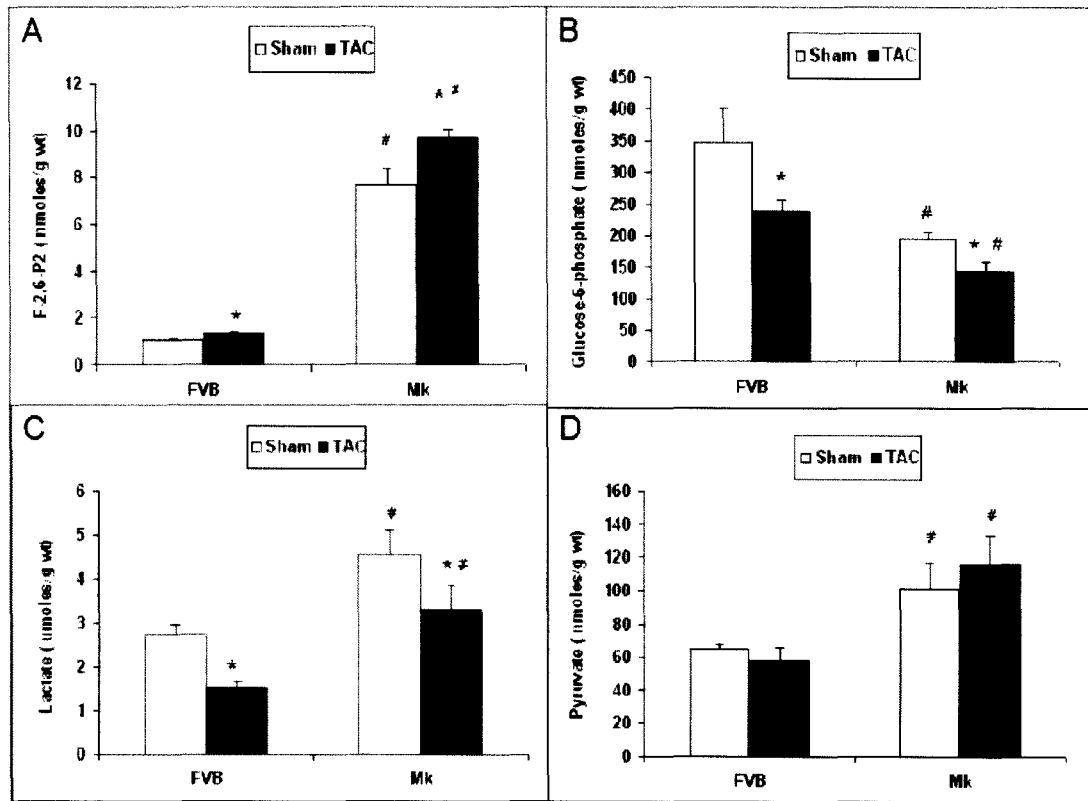


Figure 14. The content of fructose-2,6-bisphosphate (F-2,6-P₂), glucose-6-phosphate, lactate and pyruvate in FVB and Mk hearts 13 weeks after TAC. (A) Mk-sham had 6 fold higher F-2,6-P₂ content than FVB-sham. TAC increased the content of F-2,6-P₂ in both FVB and Mk hearts, however, F-2,6-P₂ content in Mk-TAC was still much higher than in FVB-TAC. (B) The glucose-6-phosphate content declined in Mk-sham. TAC decreased the level of glucose-6-phosphate in both FVB and Mk mice, with a significantly lower level of glucose-6-phosphate in Mk-TAC compared to FVB-TAC. (C) Lactate content in Mk-sham elevated significantly compared to FVB-sham. After TAC, both FVB and Mk exhibited a significant reduction of lactate, whereas the lactate content in Mk-TAC was still higher than in FVB-TAC. (D) TAC did not change the content of pyruvate in both FVB and Mk after sham and TAC surgery, however, the pyruvate content in Mk was always higher than FVB, with or without TAC. The statistical analysis was done by two way ANOVA, *, p<0.05, sham vs. TAC; #, p<0.05, Mk-sham vs. FVB-sham or Mk-TAC vs. FVB-TAC, n=5 for each group.

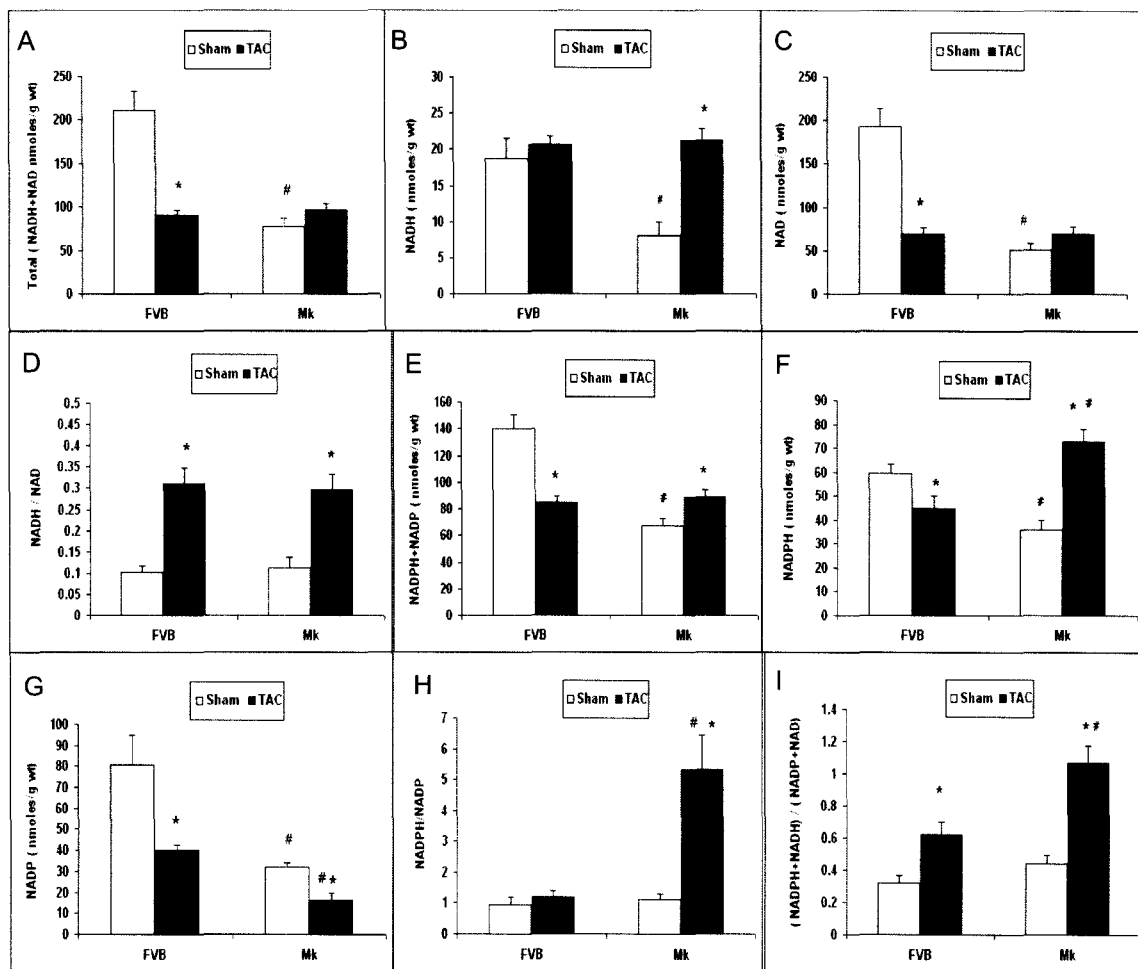


Figure 15. The content of pyridine nucleotides in FVB and Mk hearts 13 weeks after TAC. (A) The total of NADH and NAD⁺ content in Mk sham was reduced to half of that in FVB-sham. After TAC, the total content of NADH and NAD⁺ content was decreased significantly in FVB but not in Mk hearts, and no significant difference was found between FVB-TAC and Mk-TAC. (B) NADH content was similar in FVB with and without TAC. Mk-sham contained lower NADH content than FVB-sham. However, after TAC, NADH content in Mk hearts was back to levels found in FVB-sham. (C) The content of NAD⁺ in Mk-sham was significantly lower than in FVB-sham. After TAC, NAD⁺ content decreased significantly in FVB but not in Mk hearts relative to sham. No significant difference was found between FVB-TAC and Mk-TAC. (D) The ratio of NADH to NAD⁺ was similar between Mk-sham and FVB-sham. After TAC, the ratio in FVB and Mk went up significantly, whereas no significance was found when comparing FVB-TAC with Mk-TAC. (E) The total of NADPH and NADP⁺ content decreased by 50% in-Mk sham compared to FVB-sham. TAC reduced the total of NADPH and NADP⁺ content in FVB. In contrast, TAC increased the total of NADPH and NADP⁺ content in Mk, as a consequence, the content of total NADPH and NADP⁺ in Mk-TAC was similar to that in FVB-TAC. (F) NADPH level in Mk-sham was half that in FVB-sham. TAC decreased the level of NADPH in FVB hearts, conversely, TAC increased the level of NADPH in Mk hearts. Furthermore, a significant increase of NADPH content was observed in Mk-TAC compared to FVB-TAC. (G) NADP⁺ content declined in Mk-sham compared to FVB-sham. TAC decreased NADP⁺ content in both FVB and Mk hearts. As a result, NADP⁺ content in Mk-TAC was significantly lower than in FVB TAC. (H) TAC increased the ratio of NADPH to NADP⁺ in Mk compared to FVB, and

without a significant difference between Mk-sham and FVB-sham. (I) The ratio of reduced nucleotides, NADPH plus NADH, to oxidized nucleotides, NADP^+ plus NAD^+ , was significantly increased in both FVB and Mk hearts after TAC, and the ratio in Mk-TAC was significantly greater than in FVB-TAC. No significance was found between Mk-sham and FVB-sham. *, $p < 0.05$, sham vs. TAC; #, $p < 0.05$, Mk-sham vs. FVB-sham or Mk-TAC vs. FVB-TAC by two way ANOVA analysis, $n=5$ for each group.

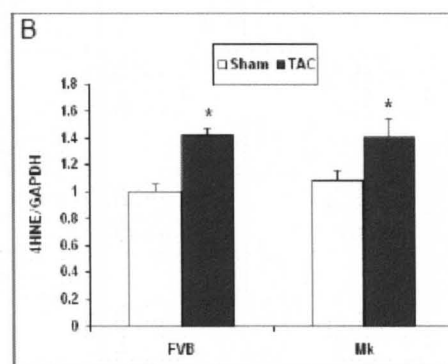
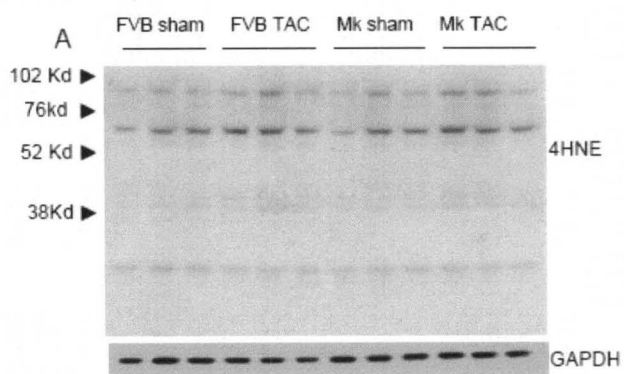


Figure 16. Oxidative stress shown by western blot for 4HNE adducts in FVB and Mk hearts 13 weeks after TAC. (A) Representative western blot picture for 4HNE adducts and GAPDH. (B) Statistical results of 4HNE adducts normalized to GAPDH. TAC increased the 4HNE adducts in both FVB and Mk hearts, without significant difference between Mk-TAC and FVB-TAC. *, $p < 0.05$, sham vs. TAC by two way ANOVA analysis, $n=6$ for each group.

CHAPTER III

CARDIAC OVEREXPRESSION OF MITOCHONDRIAL 8-OXOGUANINE DNA GLYCOSYLASE 1 PROTECTS AGAINST CARDIAC FIBROSIS FOLLOWING TRANSAORTIC CONSTRICTION

INTRODUCTION

Oxidization of DNA by reactive oxygen species (ROS) can produce nucleotide mutations potentially involved in carcinogenesis and ageing (103). Guanine is the nucleic acid base with the lowest oxidation potential, rendering it the most easily oxidizable by hydroxyl radicals and singlet oxygen (80). Therefore, oxidized guanine (7,8-dihydro-8-oxoguanine, 8-oxo-dG) is the most abundant DNA lesion following oxidative exposure. During DNA replication, 8-oxo-dG will frequently mispair with adenine, leading to formation of G:C to T:A transversions (11, 26, 64). DNA base excision is a major pathway to repair oxidized nucleotides, and the enzyme 8-oxoguanine DNA glycosylase 1 (OGG1) has a major role in the removal of 8-oxo-dG (15). For example, OGG1 deficiency in *S. cerevisiae* gives rise to a spontaneous mutator phenotype (27); A 10 fold increase of G:C to T:A transversion frequency in DNA from liver cells was found in homozygous OGG1 knock out (OGG^{-/-}) mice (46); Human OGG1 gene mutations and polymorphisms were found to be associated with head, neck, lung and kidney cancers (76, 77).

Mitochondrial DNA (mtDNA) damage is more abundant and longer lasting than nuclear DNA (nDNA) damage following exposure to oxidative stress (103, 114). A case in point is the aging rat in which levels of 8-oxo-dG in nDNA do not change from 6 to 23 months of age while 8-oxo-dG increases 2.5 fold in mtDNA with age (32) and 8-oxo-dG levels in mtDNA are an order of magnitude higher than in nDNA (29). One of the reasons that mtDNA is more sensitive to ROS mediated damage than nDNA is that mtDNA has no histone protection that can serve as a barrier against ROS. Secondly, mitochondria are the major source for superoxide production from the electron transport chain (ETC) thereby placing mtDNA in close proximity to ROS production. Lastly, mitochondria have low capacity to repair mutagenesis. The level of 8-oxo-dG in mtDNA correlates with mitochondria dysfunction in many disorders associated with oxidative stress such as ageing and neurodegeneration (62) and levels of 8-oxo-dG are inversely correlated to mammalian life span (7). Therefore, 8-oxo-dG in mtDNA is an important lesion which is at least a marker and possibly a cause for development of various diseases associated with oxidative stress.

Oxidative stress is increased in heart failure patients (37) and heart failure is frequently associated with quantitative and qualitative defects in mtDNA (42). In heart failure, mitochondria produce more superoxide than normal (100). A vicious cycle can develop for mitochondrial damage in which leakage of superoxide from the ETC promotes mtDNA damage resulting in more ETC damage which then produces more ROS and mtDNA damage. We hypothesized that this destructive cycle in the heart could be disrupted by enhancing mtDNA repair via overexpression of the repair enzyme

OGG1. To test this we produced transgenic mice with overexpression of OGG1 in cardiac mitochondria. OGG1 transgenic mice were tested for sensitivity to cardiac injury produced by transaortic constriction (TAC).

MATERIALS AND METHODS

Construction of the OGG1 transgenic mouse model with cardiac specific overexpression of mitochondrial 8-oxoguanine DNA glycosylase 1

First strand OGG1 cDNA was synthesized from human fibroblast total RNA by superscript II and oligo dT primers (Invitrogen). The cDNA was amplified by polymerase chain reaction (PCR) using primers designed for the human mitochondrial isotype of OGG1 (12, 71)(human OGG1-2a, sense primer with an additional Sal I restriction site, 5'-gacttagtcgaccgggagaagataagtcgcaa-3' and an antisense primers with an additional Hind III restriction cutting site, 5'-actactaagcttcagaggccacataatgtt-3'). This produced a 1704bp fragment lacking the nuclear localization signal of exon 7. The purified OGG1 cDNA fragment was subcloned behind a 5.5 kb DNA fragment containing the α -myosin heavy chain promoter (28) which produces transcription exclusively in cardiac myocytes and in front of a 500 bp of poly (A) DNA sequence derived from the rat insulin II gene. The sequence of the entire subcloned OGG1 cDNA fragment was confirmed. The transgene was released from the plasmid by Not I digestion and microinjected into single cell fertilized FVB mouse embryos by standard embryo microinjection procedures. All

animal procedures conformed to the National Institutes of Health *Guide for the Care and Use of Laboratory Animals* (NIH Pub. No. 85-23, Revised 1996) and were approved by the United State Department of Agriculture-certified University of Louisville animal care committee. Male mice age 90–120 days were used for subsequent experiments

Transaortic constriction (TAC) surgery and Echocardiographic Assessment of Cardiac Function

TAC surgery was performed by a modification a previously published (6) as described in chapter I of this dissertation.

Transthoracic echocardiography of the left ventricle was performed using a 15-MHz linear array transducer (15L8) interfaced with a Sequoia C512 system (Acuson) as previously described (109) and as detailed in chapter I of this dissertation.

Mitochondrial protein and mtDNA

Mitochondria were isolated by a previously described protocol (91) with modification. A fresh heart was cut into small pieces and homogenized by a motor driven Teflon pestle (Wheaton Scientific) in 5 ml of isolation buffer containing 10mM HEPES, 200mM Mannitol, 70mM sucrose and 1mM EGTA, pH 7.4. The homogenate was centrifuged at 700g for 10min at 4°C. The supernatant was moved to a new tube for centrifuging at 10000 rpm for 15min at 4°C. The pellet was collected and washed again

with isolation buffer. The final mitochondrial pellet was used to prepare mitochondrial DNA and mitochondrial protein. For extraction of mtDNA freshly isolated mitochondria were lysed and extracted by Qiagen kit (QIAprep mimiprep kit) for isolation of mtDNA. The concentration of mtDNA was determined with a Nanodrop spectrophotometer and the quality of mtDNA was confirmed by Sac II digestion and agarose gel electrophoresis. Mitochondrial protein was isolated from freshly isolated mitochondria in lysis buffer containing 2% SDS, 10% glycerol and 62.5mmol/L Tris HCl (pH 7.0), sonication and centrifuging at 12000rpm at 4°C for 15 min. The supernatant containing mitochondrial proteins was collected and the mitochondrial protein concentration was determined by the Lowry method (Pierce kit). Western blots (107) of mitochondrial protein were probed with rabbit anti hOGG1 antibody at 1:1000 dilution (Abcam) at 4°C over night. The secondary antibody was incubated with the membrane for another one hour at room temperature. Finally the antigen-antibody complexes were visualized with use of an enhanced chemiluniescence (ECL, GE healthcare) kit. Anti-cytochrome C oxidase IV (COX IV, Abcam) was used as loading control.

Assay of OGG1 activity

The fresh isolated mitochondrial pellet was lysed in buffer containing 20mM Hepes-KOH (pH 7.4), 1 mM EDTA, 1 mM DTT, 300 mM KCl, 5% glycerol, and 0.5% Triton X-100 on ice for 10min. The lysate was centrifuged at 13,000rpm for 30min at 4°C (95). The supernatant was collected and the concentration of mitochondrial protein was determined by the Lowry method. OGG1 activity in mitochondria was determined

by excising 8-oxoG from a ^{32}P -labeled oligonucleotide substrate as described (95) with modification. Briefly, a synthetic oligonucleotide containing an 8-oxoguanine adduct (5' gaactagtGatcccccggtg-3', Trevigen, cat# 3850-100-01, where O is 8-oxoguanine) was labeled with γ - ^{32}P -ATP by T4 kinase (Invitrogen) and the labeled oligonucleotide was annealed with its complementary oligonucleotide (5'-gcagccgggggatccactagttc-3', Invitrogen). Unincorporated label was removed by passage over a NAP-5 column (GE Healthcare). Fifty μg of mitochondrial protein was incubated with 0.1pmol of the ^{32}P -labeled duplex oligonucleotide in excision buffer (20 mM Hepes-KOH (pH 7.6), 5 mM EDTA, 1 mM DTT, 100 mM KCl, 5% glycerol) for 3h at 37°C in a volume of 20 μl . After incubation the reaction was terminated by addition of proteinase K (250 $\mu\text{g}/\text{ml}$) and SDS (0.5%) and heating at 50°C for 15 min. Oligonucleotides were precipitated with 70% ethanol, 45mM ammonium acetate and 0.01 $\mu\text{g}/\mu\text{l}$ glycogen and redissolved in loading buffer containing 70% formamide, 30mM NaOH and 0.05% bromophenol blue. The substrate and cleaved oligonucleotide product were separated on a gradient (4%-15%) polyacrylamide gel containing 7 M urea (Invitrogen). Radioactivity in the separated DNA bands was quantitated with a PhosphorImager and Imagequant software (Molecular Dynamics).

Real Time Polymerase Chain Reaction (RT-PCR)

Cardiac RNA was extracted with Trizol reagent. The total RNA was transcribed to cDNA with Superscript II enzyme and random oligonucleotide primers (Invitrogen).

The primers, probes and reaction buffer for RT-PCR were purchased from AB (Applied Biosystem) including hOGG1(Hs00213454_m1), α -MHC (Mm01313844_mH), β -MHC(Mm00600555_m1), ANP (Mm01255748_g1), BNP (Mm01255770_g1), procollagen 1 α 1(Mm01302043_g1), procollagen 3 α 1(Mm01254476_m1), 18s RNA (Hs99999901_s1) and 2 \times Master buffer. RT-PCR was carried out on AB 73000 thermocycler with 35 cycles, each cycle consisted of 95°C for 15 seconds, 55°C for 15 seconds and 75°C for 30 seconds. 18sRNA was used as endogenous control for other primers.

Histological experiments

Details seen described in Methods for chapter I.

Measurement of 8-oxo-dG content in mtDNA

Content of 8-oxo-dG was measured using a commercial enzyme-linked immunoassay kit (Trevigen Inc., Gaithersburg MD) as described by Gao (23) with modification. In brief, 0.5 μ g of sample mtDNA or 8-oxo-dG standards from 0 to 60ng/ml were mixed with anti-8-oxo-dG antibody overnight at 4°C, the sample mtDNA and 8-oxo-dG standards were transferred to a 96 well microplate previously coated with albumin:8-oxo-dG adduct and kept in the dark at room temperature for 2 hrs. The secondary antibody coupled with peroxidase was added to each well and an incubation followed for 1h in the dark and the plate was washed. After 6 rounds of washing, the substrate tetramethylbenzidine was added and the reaction continued for 15 min in the dark at

room temperature. A stop solution was used to end the reaction. The wavelength of 450nm was set to measure the absorbance of the final solution in each well. Results were calculated according to the standard curve.

RESULTS

Characterization of mitochondrial targeted 8-oxoguanine DNA glycosylase 1 (OGG1) transgenic mice

Transgenic mice carrying a cardiac targeted transgene for overexpression of human mitochondrial OGG1 were produced as described above in the Methods section. A total of four positive founders were obtained from 22 pups. The founder lines were named OGG1-3, OGG1-6, OGG1-7 and OGG1-10. Lines OGG1-3 and OGG1-10 were fertile and passed on the transgene to approximately 50% of offspring. These lines were tested for expression of human OGG1 mRNA and mitochondrial protein and OGG1 activity. The expression of human OGG1 mRNA in heart was significantly elevated (Figure 17A, $P < 0.01$ versus FVB control). Human OGG1 protein was markedly increased in both transgenic lines by western blot (Figure 17B). OGG1 activity measured in extracts of cardiac mitochondria was almost two fold elevated over FVB in both transgenic lines (Figure 17C, $P < 0.01$). Lines OGG1-3 and OGG1-10 had similar human OGG1 expression by all parameters, and line OGG1-10 was used for subsequent experiments. To confirm OGG1 activity in vivo, OGG1-10 mice were injected with

11mg/kg doxorubicin or saline and 8-oxo-dG content of mtDNA was measured 48 hrs post-injection. As shown in Figure 17D, doxorubicin increased 8-oxo-dG content in transgenic and control mtDNA. The OGG1 transgene produced significant reductions of 25% and 31% in 8-oxo-dG content in saline and doxorubicin treated mice, respectively. These results established the cardiac overexpression of active OGG1 in transgenic mice.

Evaluation of heart size and function

Transaortic constriction (TAC) mimics human aortic stenosis with development of pressure-overload-induced left ventricular hypertrophy. TAC or sham surgery was performed on OGG1 and FVB mice, and mice were sacrificed after 13 weeks. As shown in Table 3, TAC surgery significantly increased the ratio of heart to tibia length and heart to body weight ratio in FVB and OGG1 mice. When compared by heart to body weight ratio there was less hypertrophy in OGG1 mice ($P<0.05$). However this was partially due to differences in body weight. When heart weight was compared to tibia length, the difference in hypertrophy of OGG1 and FVB mice did not quite reach significance ($P=0.07$).

Echocardiography was used to assess the effect of TAC and the OGG1 transgene on cardiac function. The data reported in Table 4 show that TAC mice had significantly impaired cardiac function compared to sham mice. This was evident by several parameters including increased left ventricular end diastolic and systolic diameter as well as reduced ejection fraction. However there were no significant differences between

FVB and OGG1 mice, indicating that OGG1 overexpression did not alter cardiac function nor protect it from the effect of TAC.

Hypertrophic mRNA markers β -MHC, α -MHC, ANP and BNP were measured to determine whether OGG1 could reduce the fetal pattern of RNA expression induced by pressure overload and hypertrophy (Figure 18). These mRNAs were similar in OGG1 and FVB sham mice. In both OGG1 and FVB mice, TAC produced the expected increases in expression of β -MHC, ANP and BNP as well as the expected reduction in expression of α -MHC. Compared to FVB TAC mice, OGG1 TAC mice had 41% lower expression of β -MHC ($P<0.05$), and OGG1 TAC mice tended toward lower BNP expression (35% lower than FVB TAC, $P=0.12$).

TAC induction of cardiac fibrosis

Semiquantative analysis showed that 13 weeks after TAC surgery fibrosis was significantly increased in both OGG1 and FVB mice (Figures 19A and 19B, $P<0.05$). This analysis also showed that interstitial fibrosis staining was lower in OGG1 TAC mice compared to FVB TAC mice ($P<0.05$). The staining analysis was supported by RT-PCR assays of cardiac collagen mRNA expression (Figures 19C and 19D). Compared to FVB TAC mice, the expression of collagen 1 α and collagen 3 α mRNAs was 49% and 48% lower in OGG1 TAC mice, respectively ($P<0.05$ for both mRNAs).

8-oxo-dG content in mtDNA after TAC

Thirteen weeks after surgery we tested whether TAC increased 8-oxo-dG content in mtDNA and whether OGG1 overexpression could reduce mtDNA 8-oxo-dG content (Figure 20). For FVB mice, TAC produced a significant 30% increase in 8-oxo-dG ($P<0.05$). Overexpression of OGG1 essentially eliminated the ability of TAC to increase 8-oxo-dG levels. In addition, OGG1 sham mice had 25% lower 8-oxo-dG content than FVB sham ($P<0.05$). These results show that OGG1 provides protection against some components of cardiac failure in the TAC model including reduction in fibrosis, β -MHC expression and 8-oxo-dG content in mtDNA.

DISCUSSION

Damage to cardiac mtDNA by reactive oxygen has been proposed to contribute to the development of heart failure (7, 42, 99). Human studies (42) and animal models (21, 52, 75, 88) have demonstrated that there is a strong association between cardiac injury and oxidative damage to mtDNA. This relationship has been shown following numerous different treatments including exposure to doxorubicin ((52, 88), angiotensin (81), or isoproterenol (45), the process of ageing (14, 32), and knockout out of mitochondrial SOD2 (63). However no cardiac-specific models have been created to determine if reducing mtDNA damage can protect the heart, thereby testing whether the association between oxidative mtDNA damage and heart failure is actually a causal relationship. In this chapter, we describe successful production of OGG1 transgenic mice, which have

cardiac-specific overexpression of active mitochondrial OGG1 enzyme which catalyses the first essential step in the repair pathway of oxidized mtDNA. OGG1 transgenic mice were shown to have increased hOGG1 mRNA, elevated hOGG1 protein and a 2 fold increase in OGG1 enzyme activity in mitochondria. In vivo efficacy of the transgene was demonstrated by reduced levels of mitochondrial 8-oxo-dG content under basal conditions, after doxorubicin treatment and after TAC surgery. Overexpression of OGG1 produced no measurable detrimental effects on the heart. Thus this transgenic line provides a suitable model for performing direct tests of a causal role for mtDNA mutations in cardiac pathology.

The efficacy of OGG1 overexpression in a heart failure model was tested by challenge with TAC surgery. Transgenic mice demonstrated essentially complete protection from TAC induced elevation of 8-oxo-dG content, but despite this protection, we saw little benefit of the OGG1 transgene either to reduce cardiac hypertrophy or to improve cardiac function measured by echocardiography 13 weeks after surgery. There are multiple potential explanations for this lack of effect. One explanation may be that the growth factor pathways(30) or kinase mediated actin rearrangement (50, 56) activated by mechanical stress on the heart contributing to cardiac hypertrophy and dysfunction are not closely linked to the condition of mtDNA. If these pathways are not linked to mtDNA condition, then the reduction in mtDNA mutations produced by the OGG1 transgene cannot protect from TAC induced hypertrophy. However, the fact that OGG1 transgenic mice had reduced β -MHC mRNA expression after TAC suggests that mtDNA mutations have at least a modest impact on the cardiac hypertrophy response. An

alternative reason for the lack of a larger OGG1 effect may be that we did not wait long enough after surgery. The 13 week time point after TAC may not be long enough for sufficient mtDNA mutation to accumulate and disrupt mitochondrial function. Over a longer period, mutated mtDNA may spread within individual myocytes from heteroplasmy towards homoplasmy through a mechanism called “relaxed replication” (14). Accumulation of mtDNA mutations appears to have a high threshold before essential mitochondrial functions are compromised: In OGG1^{-/-} mice elevation of 8-oxo-dG content in mtDNA did not produce a measurable impairment of mitochondrial function in heart or liver (93). Potentially more time after TAC surgery or ageing studies may be more appropriate to reveal the full benefit of the OGG1 transgene.

Apart from decreased mitochondrial 8-oxo-dG, the principle benefit of OGG1 overexpression was a significant decrease in TAC induced cardiac fibrosis. This protection was indicated by reduced Sirius Red staining on OGG1 cardiac sections, was confirmed by decreased induction of collagen 1 and 3 mRNA expression in OGG1 hearts after TAC surgery. Cardiac fibrosis is primarily mediated by collagen secreting myofibroblasts (102). Myofibroblasts cannot overexpress OGG1 due to regulation of the transgene by the cardiomyocyte specific α -MHC promoter (2). Therefore, cardiomyocyte overexpression of OGG1 apparently decreased a pro-fibrotic signal that originated in TAC stressed cardiomyocytes and acted on myofibroblasts to stimulate production of collagen matrix. It is surprising that the OGG1 transgene had only a small effect on cardiac hypertrophy but had a large effect on fibrosis. This may imply that the pro-fibrotic signaling process is more sensitive to mtDNA oxidation than is the hypertrophic

response. Alternatively, the fact that many myofibroblasts can be stimulated by a diffusible molecule may result in amplification of the pro-fibrotic signal from just the most damaged cardiomyocytes. The anti-fibrotic effects of the OGG1 transgene may be due to protection of mtDNA resulting in production of fewer severely injured cardiomyocytes or less pro-fibrotic signaling from these cardiomyocytes.

In summary, cardiac overexpression of mitochondrial OGG1 reduced mtDNA content of 8-oxo-dG in normal and stressed hearts. After TAC, protection of mtDNA slightly reduced the hypertrophic response and clearly decreased cardiac fibrosis. These findings support the concept that mtDNA oxidation has a causal role in cardiac damage.

Table 3. Measurement of heart weight, body weight, tibia length and the ratios of heart weight to body weight and to tibia length in FVB and OGG1 mice 13 weeks after TAC or sham surgery.

Parameters	FVB-sham	FVB-TAC	OGG1-sham	OGG1-TAC
Heart weight (mg)	124.8±2.9	186.9±9.1 ^a	128.9±3.0	168.8±8.0 ^a
Body weight (g)	30.8±0.9	31.8±0.7	31.8±0.7	33.7±1.0
Tibia length (mm)	18.14±0.16	18.29±0.07	18.24±0.07	18.32±0.07
HW/BW	4.09±0.15	5.91±0.31 ^a	4.01±0.14	5.09±0.32 ^{a,b}
HW/TL	6.88±0.14	10.22±0.50 ^a	7.07±0.16	9.22±0.45 ^a

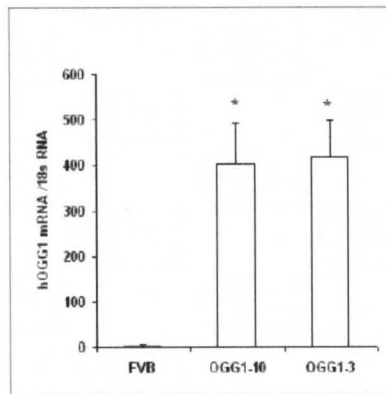
Legend: The notation a indicates $P < 0.05$, FVB-sham vs. FVB-TAC or OGG1-sham vs. OGG1-TAC. The notation b indicates $P < 0.05$, OGG1-TAC vs. FVB-TAC by two way ANOVA analysis, $n=11$ for sham and $n=14$ for TAC groups. HW/BW, the heart weight to body weight ratio; HW/TL, the heart weight to tibia length ratio.

**Table 4. Cardiac function measured by echocardiography in FVB and OGG1 mice
13 weeks after TAC or sham surgery.**

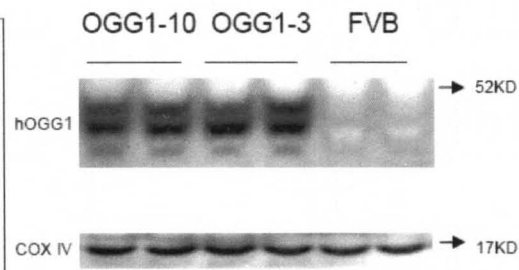
Parameter	FVB-Sham	FVB-TAC	OGG1-Sham	OGG1-TAC
LVEDD (mm)	3.81±0.08	4.15±0.05 ^a	3.81±0.10	4.03±0.08 ^a
LVESD (mm)	2.36±0.10	2.76±0.08 ^a	2.27±0.09	2.59±0.08 ^a
IVS (d) (mm)	0.91±0.02	1.02±0.03 ^a	0.89±0.03	1.0±0.02 ^a
IVS (s) (mm)	1.18±0.03	1.29±0.03 ^a	1.19±0.03	1.24±0.02
PWTh (d) (mm)	0.80±0.04	0.89±0.03 ^a	0.76±0.03	0.84±0.03
PWTh (s) (mm)	1.16±0.04	1.25±0.02	1.17±0.05	1.25±0.03
IVS%Th	30.87±2.78	29.26±3.50	33.74±2.67	24.72±2.73
PW%Th	40.67±5.27	40.32±3.08	48.51±3.31	49.03±4.08
IVS/PW	1.16±0.05	1.13±0.03	2.2±1.01	1.19±0.04
%FS	38.6±1.7	33.8±1.1 ^a	40.59±1.40	34.47±1.06 ^a
HR (beats/min)	487±10	516±11	513±12	535±12

Legend: Data are mean \pm SE. a, $p<0.05$, FVB sham vs. FVB TAC or OGG1 sham vs. OGG1 TAC by two way ANOVA analysis, n=12 for FVB sham, n=10 for OGG1 sham, n=14 for FVB TAC and n=13 for OGG1 TCA group. LVEDD, left ventricular end diastolic diameter; LVESD, left ventricular end systolic diameter; IVS(d), interventricular septum thickness at diastole; IVS(s), interventricular septum thickness at systole; PWTh(d), post wall thickness at diastole; PWTh(s), post wall thickness at systole; IVS%Th, interventricular septum % thickening; PW%Th, posterior wall % thickening; IVS/PW, interventricular septum to posterior wall thickness ratio; %FS, percent fractional shortening; EF, ejection fraction; HR, heart rates.

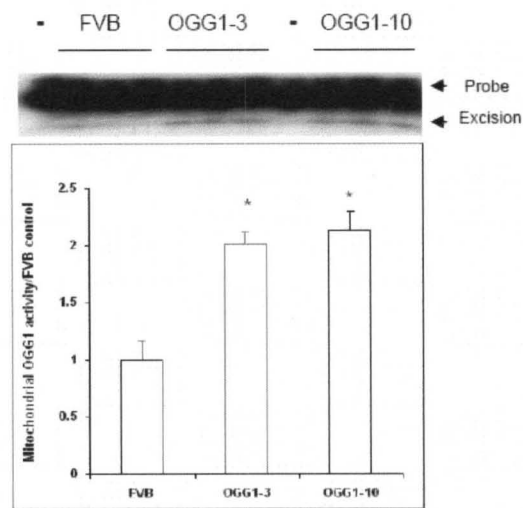
A



B



C



D

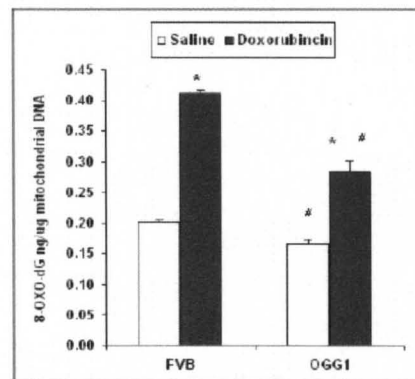


Figure 17. Elevation of OGG1 mRNA, protein and enzyme activity in OGG1 transgenic mice. (A) hOGG1 mRNA level, detected by RT-PCR in cardiac RNA of OGG1-10 and OGG1-3 mice was significantly increased versus FVB control (*, $P<0.001$ vs. FVB control by one way ANOVA analysis, $n=5$ for each group). (B) Western blot of expression of hOGG1 protein in isolated mitochondria. No hOGG1 band was detected in FVB control mice in contrast to strong bands for the two OGG1 lines. COX IV was used as loading control. (C) OGG1 enzyme activity was measured by cleavage of a ^{32}P end labeled, 8-oxo-dG containing oligonucleotide substrate using 50 μg of mitochondrial protein (Probe, ^{32}P end labeled oligonucleotide containing 8-oxo-dG; Excision, excised probe; -, no protein added as blank control). The activity of OGG1 in the two lines was almost 2 fold higher than that of FVB control (*, $p<0.01$, vs. FVB control by one way ANOVA analysis, $n=6$ for each group). (D) Content of 8-oxo-dG in mtDNA from mice 48 hr after treatment with 11mg/kg doxorubicin. Doxorubicin increased 8-oxo-dG content ($P<0.05$) in FVB and OGG1 mice. The OGG1 transgene reduced 8-oxo-dG content in saline and doxorubicin treated mice ($P<0.05$). Statistical analysis of 8-oxo-dG content was performed with two way ANOVA analysis, $n=5$ for each group.

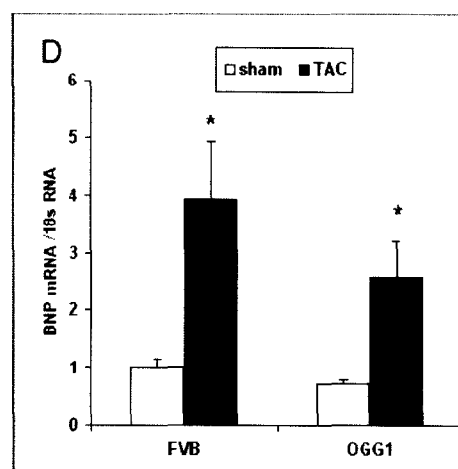
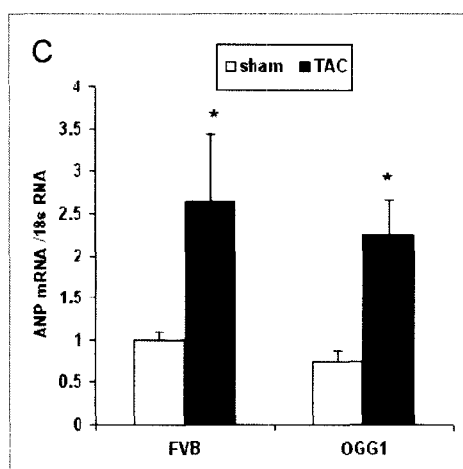
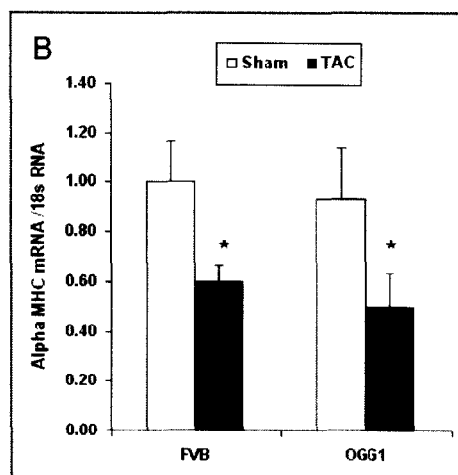
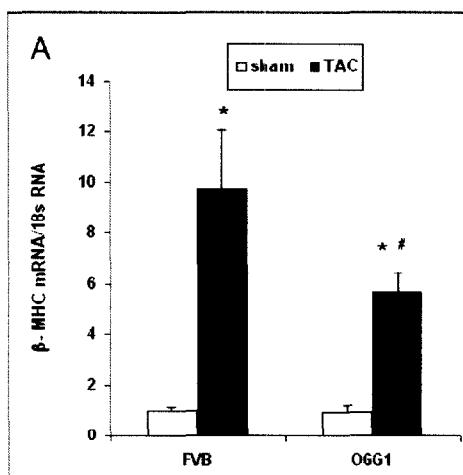


Figure 18. Hypertrophic biomarkers β -MHC, α -MHC, ANP and BNP mRNA were analyzed by RT-PCR in OGG1 and FVB hearts 13 weeks after TAC or sham surgery. (A) β -MHC mRNA was significantly increased after TAC in both FVB and OGG1 hearts, however, the β -MHC mRNA level in OGG1 TAC hearts was significantly lower than that in FVB TAC hearts. (B) α -MHC mRNA level was significantly decreased in both FVB and OGG1 after TAC and no significant difference was found between FVB and OGG1 mice with or without TAC. (C) ANP mRNA and (D) BNP mRNA were increased significantly after TAC compared with sham mice. No significant difference was found between OGG1 and FVB in sham or TAC groups. Statistical analysis was done by two way ANOVA. *, $p < 0.05$, Sham vs. TAC; #, $p < 0.05$, OGG1 TAC vs. FVB TAC, $n=5$ for FVB sham, FVB TAC and OGG1 sham, $n=8$ for OGG1 TAC.

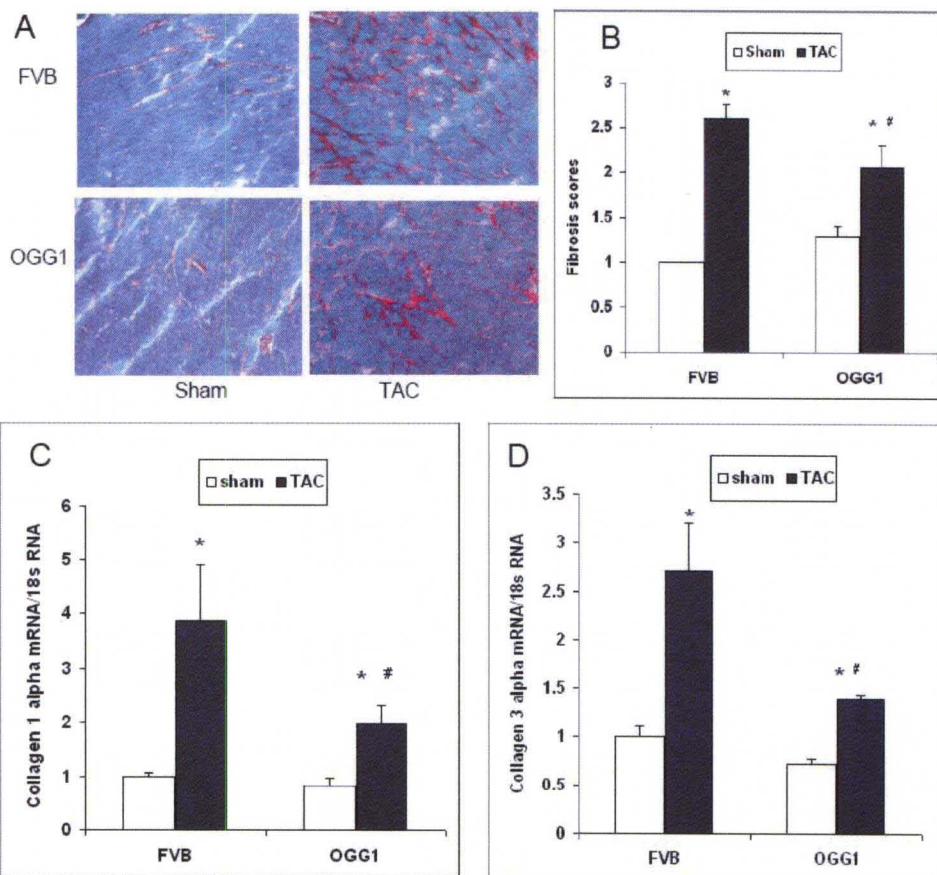


Figure 19. Fibrosis in FVB and OGG1 hearts 13 weeks after TAC. (A)

Representative sirius red staining for fibrosis in FVB and OGG1 hearts. (B) Semi quantitative scores for fibrosis staining performed as described in Methods by a blinded observer. Staining of fibrosis in OGG1 TAC hearts was significantly lower than that in FVB TAC hearts (#, $p<0.05$, OGG1 TAC vs. FVB TAC; *, $p<0.05$, Sham vs. TAC by two way ANOVA, $n=5$ for each group). The expression of collagen 1 α 1 mRNA (panel C) and collagen 3 α 1 mRNA (panel D) measured by RT-PCR was significantly lower in OGG1 TAC hearts than in FVB TAC hearts (#, $P<0.05$, OGG1 TAC vs. FVB TAC and *, $P<0.05$, Sham vs. TAC by 2-way ANOVA, $n=5$ for FVB sham, FVB TAC and OGG1 sham, $n=8$ for OGG1 TAC).

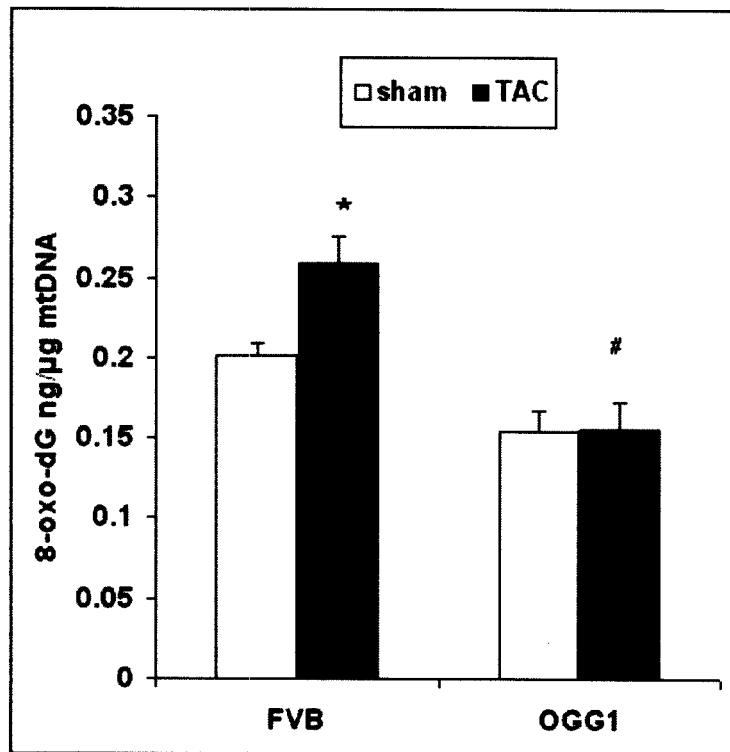


Figure 20. Content of 8-oxo-dG content in mtDNA 13 weeks after TAC. TAC increased 8-oxo-dG content in FVB mice (*, $P < 0.05$ for FVB sham vs. FVB TAC). OGG1 lowered sham levels of 8-oxo-dG and prevented the TAC induced increase in 8-oxo-dG content (#, $P < 0.05$ for OGG1 sham vs. FVB sham and for OGG1 TAC vs. FVB TAC, all statistics by two way ANOVA, $n=6$ for each group).

CHAPTER IV

OVERVIEW AND RELEVANCE OF DISSERTATION

Review of results

Hearts with either reduced or increased glycolysis exhibited several indications of greater damage after TAC surgery. This included: More severe cardiac structural changes including greater hypertrophy with fibrosis, greater functional changes evident as reduced fractional shortening and increased lung weight to tibia length ratio, lower energy reserves and higher reductive status. However, only Mb transgenic hearts with reduced glycolysis displayed increased oxidative stress.

The OGG1 transgene which expresses the mitochondrial DNA repair enzyme 8-oxoguanine DNA glycosylase 1 provided partial protection against the damaging effects of TAC surgery. This was evident as reduced fibrosis 13 weeks after TAC surgery and reduction of 8-oxo-dG content in mtDNA.

Significance of pathology to heart failure

The results from all lines of mice implicated mitochondrial dysfunction and oxidative stress in the pathogenesis of heart failure. Mitochondria are the major energy source of the cell and reduced energy reserves (PCr/ATP ratio) were a characteristic of both Mb and Mk hearts after TAC surgery. Mitochondria are also the major cellular

source of reactive oxygen species, and the oxidative stress markers 8-oxo-dG and HNE-protein adducts were increased in both transgenic and non-transgenic TAC hearts. Mb-TAC hearts, in particular, appeared to have the highest level of oxidative stress as indicated by the fact that they had the highest levels of HNE-protein adducts. The reasons for increased mitochondrial dysfunction in Mk- and Mb-TAC hearts may be different. In Mb hearts, lower glycolysis could be compensated for by an increase of fatty acid oxidation according to the theory of the Randle Cycle. Higher fatty acid oxidation induces higher ROS production in mitochondria. In Mk mice, with higher glycolysis mitochondrial dysfunction could be derived from glucotoxicity, possibly from more substrates entering the AGE (advanced glycosylation end products) and PKC (protein kinase C) pathways in the distal half of the glycolytic pathway. In OGG1 mice DNA in mitochondria was protected and OGG1 proved to be the only transgene that was partially protective against heart failure. Thus Mb and Mk transgenes that increased mitochondrial damage worsened heart failure and the OGG1 transgene, which protected mitochondria reduced heart failure.

The most significant finding from Mb and Mk mice was that inhibiting the ability of the heart to modulate glycolysis, either up or down, renders the heart more susceptible to the stress induced by pressure overload. A possible explanation was that both Mb- and Mk-TAC hearts showed decreased content of NADP^+ , which promoted higher reductive status. There are many enzymes which are dependent on NADP^+ such as isocitrate NADP^+ dependent dehydrogenase. A decrease in NADP^+ content could affect the activities of NADP^+ -dependent enzymes and this could affect cardiac function. NADP^+

content is associated with calcium signaling , and abnormal NADP⁺ content probably causes abnormal calcium signaling (47), which could cause cardiac hypertrophy (78). Regardless of the specific mechanism, neither Mk nor Mb induced cardiac damage unless the heart was exposed to pressure overload. This indicates that under normal conditions the heart is able to compensate for significant changes in metabolism.

Clinical relevance

Ultimately the aim of this work is to better understand and thereby enhance our ability to treat patients with cardiac dysfunction. A beneficial aspect of higher glycolysis in Mk-TAC hearts was increased content of NADPH, which is important as an antioxidant agent. However, the higher NADPH content could not prevent severer cardiac structural and functional changes induced by TAC. This suggests that anti-oxidant drugs alone may not be able to completely protect the heart. The data from the OGG1 transgenic mice suggest that oxidation of mtDNA could result in higher fibrosis, which is associated with cardiac remodeling, thus anti oxidant drugs that provide protection of mtDNA against ROS may be useful for the prevention or treatment of heart failure.

Several candidate drugs are available or in development to treat angina, ischemic heart diseases, heart failure and diabetic heart diseases by changing metabolism through shifting fatty acid oxidation to glucose oxidation (74). These include trimetazidine, ranolazine, perhexiline and etomoxir. Trimetazidine , an anti angina agent, decreases fatty acid oxidation by inhibiting 3-ketoacyl coenzyme A thiolase, thereby relieving inhibition of pyruvate dehydrogenase activity and correspondingly increasing glucose

oxidation (74). This anti-angina agent can relieve symptoms due to oxygen sparing effects and reduced intracellular acidosis and calcium overload, probably through coupling glycolysis and glucose oxidation. However, according to our results, permanently manipulating cardiac metabolism, either by increasing or decreasing glycolysis, is detrimental and increases heart failure. The same concerns apply to each of the candidate drugs that are proposed to benefit the heart by changing cardiac metabolism. Therefore great care should be taken before long term application of these drugs to heart failure patients.

Future studies

Future studies are needed to understand the specific changes in mitochondrial function in Mk, Mb and OGG hearts. It should be determined whether mitochondrial respiration efficiency is altered, whether changes are present in the electron transport chain and it should be tested if the amounts of superoxide produced is increased. We should also test whether these transgenes produce similar changes in heart dysfunction using different models of heart failure or damage. These models could include chronic stress in the heart with known hypertrophic agents, such as angiotensin II and phenylephrine. The effects of altering glycolysis may be especially relevant to diabetic cardiomyopathy in which changes in fuel use are likely to be a major component of the cardiac pathology. Since human ageing is associated with mutations of mtDNA the OGG1 gene would be especially useful for studying cardiac aging. The OGG1 transgene had lower base line of oxidized guanine, thus the OGG1 transgene would be predicted to decrease the detrimental effects of aging on cardiac function.

REFERENCES

1. Abel ED, Kaulbach HC, Tian R, Hopkins JC, Duffy J, Doetschman T, Minnemann T, Boers ME, Hadro E, Oberste-Berghaus C, Quist W, Lowell BB, Ingwall JS, and Kahn BB. Cardiac hypertrophy with preserved contractile function after selective deletion of GLUT4 from the heart. *J Clin Invest* 104: 1703-1714, 1999.
2. Aikawa R, Huggins GS, and Snyder RO. Cardiomyocyte-specific gene expression following recombinant adeno-associated viral vector transduction. *J Biol Chem* 277: 18979-18985, 2002.
3. Allard MF, Schonekess BO, Henning SL, English DR, and Lopaschuk GD. Contribution of oxidative metabolism and glycolysis to ATP production in hypertrophied hearts. *Am J Physiol* 267: H742-750, 1994.
4. Aon MA, Cortassa S, and O'Rourke B. Redox-optimized ROS balance: a unifying hypothesis. *Biochim Biophys Acta* 1797: 865-877, 2010.
5. Aragno M, Mastrocola R, Medana C, Catalano MG, Vercellinatto I, Danni O, and Boccuzzi G. Oxidative stress-dependent impairment of cardiac-specific transcription factors in experimental diabetes. *Endocrinology* 147: 5967-5974, 2006.
6. Arany Z, Novikov M, Chin S, Ma Y, Rosenzweig A, and Spiegelman BM. Transverse aortic constriction leads to accelerated heart failure in mice lacking PPAR-gamma coactivator 1alpha. *Proc Natl Acad Sci U S A* 103: 10086-10091, 2006.
7. Barja G, and Herrero A. Oxidative damage to mitochondrial DNA is inversely related to maximum life span in the heart and brain of mammals. *FASEB J* 14: 312-318, 2000.
8. Bernofsky C, and Swan M. An improved cycling assay for nicotinamide adenine dinucleotide. *Anal Biochem* 53: 452-458, 1973.
9. Bishop SP, and Altschuld RA. Increased glycolytic metabolism in cardiac hypertrophy and congestive failure. *Am J Physiol* 218: 153-159, 1970.
10. Bogoyevitch MA, Glennon PE, Andersson MB, Clerk A, Lazou A, Marshall CJ, Parker PJ, and Sugden PH. Endothelin-1 and fibroblast growth factors stimulate the mitogen-activated protein kinase signaling cascade in cardiac myocytes. The potential role of the cascade in the integration of two signaling pathways leading to myocyte hypertrophy. *J Biol Chem* 269: 1110-1119, 1994.

11. Boiteux S, and Radicella JP. Base excision repair of 8-hydroxyguanine protects DNA from endogenous oxidative stress. *Biochimie* 81: 59-67, 1999.
12. Boiteux S, and Radicella JP. The human OGG1 gene: structure, functions, and its implication in the process of carcinogenesis. *Arch Biochem Biophys* 377: 1-8, 2000.
13. Brownlee M. Biochemistry and molecular cell biology of diabetic complications. *Nature* 414: 813-820, 2001.
14. Chinnery PF, Samuels DC, Elson J, and Turnbull DM. Accumulation of mitochondrial DNA mutations in ageing, cancer, and mitochondrial disease: is there a common mechanism? *Lancet* 360: 1323-1325, 2002.
15. de Souza-Pinto NC, Eide L, Hogue BA, Thybo T, Stevnsner T, Seeberg E, Klungland A, and Bohr VA. Repair of 8-oxodeoxyguanosine lesions in mitochondrial dna depends on the oxoguanine dna glycosylase (OGG1) gene and 8-oxoguanine accumulates in the mitochondrial dna of OGG1-defective mice. *Cancer Res* 61: 5378-5381, 2001.
16. Depre C, Rider MH, and Hue L. Mechanisms of control of heart glycolysis. *Eur J Biochem* 258: 277-290, 1998.
17. Doenst T, Pytel G, Schrepper A, Amorim P, Farber G, Shingu Y, Mohr FW, and Schwarzer M. Decreased rates of substrate oxidation ex vivo predict the onset of heart failure and contractile dysfunction in rats with pressure overload. *Cardiovasc Res* 86: 461-470, 2010.
18. Domenighetti AA, Danes VR, Curl CL, Favalaro JM, Proietto J, and Delbridge LM. Targeted GLUT-4 deficiency in the heart induces cardiomyocyte hypertrophy and impaired contractility linked with Ca(2+) and proton flux dysregulation. *J Mol Cell Cardiol* 48: 663-672, 2010.
19. Donthi RV, Ye G, Wu C, McClain DA, Lange AJ, and Epstein PN. Cardiac expression of kinase-deficient 6-phosphofructo-2-kinase/fructose-2,6-bisphosphatase inhibits glycolysis, promotes hypertrophy, impairs myocyte function, and reduces insulin sensitivity. *J Biol Chem* 279: 48085-48090, 2004.
20. Entman ML, Bornet EP, Van Winkle WB, Goldstein MA, and Schwartz A. Association of glycogenolysis with cardiac sarcoplasmic reticulum: II. Effect of glycogen depletion, deoxycholate solubilization and cardiac ischemia: evidence for a phosphorylase kinase membrane complex. *J Mol Cell Cardiol* 9: 515-528, 1977.
21. Ferreira AL, Salvadori DM, Nascimento MC, Rocha NS, Correa CR, Pereira EJ, Matsubara LS, Matsubara BB, and Ladeira MS. Tomato-oleoresin supplement prevents doxorubicin-induced cardiac myocyte oxidative DNA damage in rats. *Mutat Res* 631: 26-35, 2007.

22. Gamble J, and Lopaschuk GD. Glycolysis and glucose oxidation during reperfusion of ischemic hearts from diabetic rats. *Biochim Biophys Acta* 1225: 191-199, 1994.
23. Gao X, Campian JL, Qian M, Sun XF, and Eaton JW. Mitochondrial DNA damage in iron overload. *J Biol Chem* 284: 4767-4775, 2009.
24. Gertz EW, Wisneski JA, Stanley WC, and Neese RA. Myocardial substrate utilization during exercise in humans. Dual carbon-labeled carbohydrate isotope experiments. *J Clin Invest* 82: 2017-2025, 1988.
25. Glitsch HG, and Tappe A. The Na⁺/K⁺ pump of cardiac Purkinje cells is preferentially fuelled by glycolytic ATP production. *Pflugers Arch* 422: 380-385, 1993.
26. Grollman AP, and Moriya M. Mutagenesis by 8-oxoguanine: an enemy within. *Trends Genet* 9: 246-249, 1993.
27. Guibourt N, and Boiteux S. Expression of the Fpg protein of *Escherichia coli* in *Saccharomyces cerevisiae*: effects on spontaneous mutagenesis and sensitivity to oxidative DNA damage. *Biochimie* 82: 59-64, 2000.
28. Gulick J, Subramaniam A, Neumann J, and Robbins J. Isolation and characterization of the mouse cardiac myosin heavy chain genes. *J Biol Chem* 266: 9180-9185, 1991.
29. Hamilton ML, Van Remmen H, Drake JA, Yang H, Guo ZM, Kewitt K, Walter CA, and Richardson A. Does oxidative damage to DNA increase with age? *Proc Natl Acad Sci U S A* 98: 10469-10474, 2001.
30. Hill JA, and Olson EN. Cardiac plasticity. *N Engl J Med* 358: 1370-1380, 2008.
31. Hoek JB, and Rydstrom J. Physiological roles of nicotinamide nucleotide transhydrogenase. *Biochem J* 254: 1-10, 1988.
32. Hudson EK, Hogue BA, Souza-Pinto NC, Croteau DL, Anson RM, Bohr VA, and Hansford RG. Age-associated change in mitochondrial DNA damage. *Free Radic Res* 29: 573-579, 1998.
33. Hue L, Beauloye C, Marsin AS, Bertrand L, Horman S, and Rider MH. Insulin and ischemia stimulate glycolysis by acting on the same targets through different and opposing signaling pathways. *J Mol Cell Cardiol* 34: 1091-1097, 2002.
34. Hue L, and Taegtmeyer H. The Randle cycle revisited: a new head for an old hat. *Am J Physiol Endocrinol Metab* 297: E578-591, 2009.

35. Huggins CE, Domenighetti AA, Ritchie ME, Khalil N, Favalaro JM, Proietto J, Smyth GK, Pepe S, and Delbridge LM. Functional and metabolic remodelling in GLUT4-deficient hearts confers hyper-responsiveness to substrate intervention. *J Mol Cell Cardiol* 44: 270-280, 2008.
36. Ide T, Tsutsui H, Hayashidani S, Kang D, Suematsu N, Nakamura K, Utsumi H, Hamasaki N, and Takeshita A. Mitochondrial DNA damage and dysfunction associated with oxidative stress in failing hearts after myocardial infarction. *Circ Res* 88: 529-535, 2001.
37. Ide T, Tsutsui H, Kinugawa S, Suematsu N, Hayashidani S, Ichikawa K, Utsumi H, Machida Y, Egashira K, and Takeshita A. Direct evidence for increased hydroxyl radicals originating from superoxide in the failing myocardium. *Circ Res* 86: 152-157, 2000.
38. Ingwall JS. Energy metabolism in heart failure and remodelling. *Cardiovasc Res* 81: 412-419, 2009.
39. James J, Martin L, Krenz M, Quatman C, Jones F, Klevitsky R, Gulick J, and Robbins J. Forced expression of alpha-myosin heavy chain in the rabbit ventricle results in cardioprotection under cardiomyopathic conditions. *Circulation* 111: 2339-2346, 2005.
40. Kaczmarczyk SJ, Andrikopoulos S, Favalaro J, Domenighetti AA, Dunn A, Ernst M, Grail D, Fodero-Tavoletti M, Huggins CE, Delbridge LM, Zajac JD, and Proietto J. Threshold effects of glucose transporter-4 (GLUT4) deficiency on cardiac glucose uptake and development of hypertrophy. *J Mol Endocrinol* 31: 449-459, 2003.
41. Kagaya Y, Kanno Y, Takeyama D, Ishide N, Maruyama Y, Takahashi T, Ido T, and Takishima T. Effects of long-term pressure overload on regional myocardial glucose and free fatty acid uptake in rats. A quantitative autoradiographic study. *Circulation* 81: 1353-1361, 1990.
42. Karamanlidis G, Nascimben L, Couper GS, Shekar PS, del Monte F, and Tian R. Defective DNA replication impairs mitochondrial biogenesis in human failing hearts. *Circ Res* 106: 1541-1548.
43. Kashiwaya Y, Sato K, Tsuchiya N, Thomas S, Fell DA, Veech RL, and Passonneau JV. Control of glucose utilization in working perfused rat heart. *Journal of Biological Chemistry* 269: 25502-25514, 1994.
44. Keith M, Geranmayegan A, Sole MJ, Kurian R, Robinson A, Omran AS, and Jeejeebhoy KN. Increased oxidative stress in patients with congestive heart failure. *J Am Coll Cardiol* 31: 1352-1356, 1998.

45. Kim T, Thu VT, Han IY, Youm JB, Kim E, Kang SW, Kim YW, Lee JH, and Joo H. Does strong hypertrophic condition induce fast mitochondrial DNA mutation of rabbit heart? *Mitochondrion* 8: 279-283, 2008.
46. Klungland A, Rosewell I, Hollenbach S, Larsen E, Daly G, Epe B, Seeberg E, Lindahl T, and Barnes DE. Accumulation of premutagenic DNA lesions in mice defective in removal of oxidative base damage. *Proc Natl Acad Sci U S A* 96: 13300-13305, 1999.
47. Koch-Nolte F, Haag F, Guse AH, Lund F, and Ziegler M. Emerging roles of NAD⁺ and its metabolites in cell signaling. *Sci Signal* 2: mr1, 2009.
48. Kockskamper J, Zima AV, and Blatter LA. Modulation of sarcoplasmic reticulum Ca²⁺ release by glycolysis in cat atrial myocytes. *J Physiol* 564: 697-714, 2005.
49. Kudo N, Barr AJ, Barr RL, Desai S, and Lopaschuk GD. High rates of fatty acid oxidation during reperfusion of ischemic hearts are associated with a decrease in malonyl-CoA levels due to an increase in 5'-AMP-activated protein kinase inhibition of acetyl-CoA carboxylase. *J Biol Chem* 270: 17513-17520, 1995.
50. Kuppuswamy D, Kerr C, Narishige T, Kasi VS, Menick DR, and Cooper Gt. Association of tyrosine-phosphorylated c-Src with the cytoskeleton of hypertrophying myocardium. *J Biol Chem* 272: 4500-4508, 1997.
51. Kusuoka H, and Marban E. Mechanism of the diastolic dysfunction induced by glycolytic inhibition. Does adenosine triphosphate derived from glycolysis play a favored role in cellular Ca²⁺ homeostasis in ferret myocardium? *J Clin Invest* 93: 1216-1223, 1994.
52. Lebrecht D, Setzer B, Ketelsen UP, Haberstroh J, and Walker UA. Time-dependent and tissue-specific accumulation of mtDNA and respiratory chain defects in chronic doxorubicin cardiomyopathy. *Circulation* 108: 2423-2429, 2003.
53. Liao R, Jain M, Cui L, D'Agostino J, Aiello F, Luptak I, Ngoy S, Mortensen RM, and Tian R. Cardiac-specific overexpression of GLUT1 prevents the development of heart failure attributable to pressure overload in mice. *Circulation* 106: 2125-2131, 2002.
54. Losito VA, Tsushima RG, Diaz RJ, Wilson GJ, and Backx PH. Preferential regulation of rabbit cardiac L-type Ca²⁺ current by glycolytic derived ATP via a direct allosteric pathway. *J Physiol* 511 (Pt 1): 67-78, 1998.
55. Lowry OH, and Passonneau JV. *A flexible system of enzymatic analysis*. New York: Academic, 1993.
56. Lu H, Fedak PW, Dai X, Du C, Zhou YQ, Henkelman M, Mongroo PS, Lau A, Yamabi H, Hinek A, Husain M, Hannigan G, and Coles JG. Integrin-linked kinase

expression is elevated in human cardiac hypertrophy and induces hypertrophy in transgenic mice. *Circulation* 114: 2271-2279, 2006.

57. Lu Z, Xu X, Hu X, Lee S, Traverse JH, Zhu G, Fassett J, Tao Y, Zhang P, dos Remedios C, Pritzker M, Hall JL, Garry DJ, and Chen Y. Oxidative stress regulates left ventricular PDE5 expression in the failing heart. *Circulation* 121: 1474-1483, 2010.
58. Luiken JJ, Coort SL, Koonen DP, van der Horst DJ, Bonen A, Zorzano A, and Glatz JF. Regulation of cardiac long-chain fatty acid and glucose uptake by translocation of substrate transporters. *Pflugers Arch* 448: 1-15, 2004.
59. Luiken JJ, Schaap FG, van Nieuwenhoven FA, van der Vusse GJ, Bonen A, and Glatz JF. Cellular fatty acid transport in heart and skeletal muscle as facilitated by proteins. *Lipids* 34 Suppl: S169-175, 1999.
60. Luptak I, Yan J, Cui L, Jain M, Liao R, and Tian R. Long-term effects of increased glucose entry on mouse hearts during normal aging and ischemic stress. *Circulation* 116: 901-909, 2007.
61. Madias NE. Lactic acidosis. *Kidney Int* 29: 752-774, 1986.
62. Mandavilli BS, Santos JH, and Van Houten B. Mitochondrial DNA repair and aging. *Mutat Res* 509: 127-151, 2002.
63. Melov S, Coskun P, Patel M, Tuinstra R, Cottrell B, Jun AS, Zastawny TH, Dizdaroglu M, Goodman SI, Huang TT, Miziorko H, Epstein CJ, and Wallace DC. Mitochondrial disease in superoxide dismutase 2 mutant mice. *Proc Natl Acad Sci U S A* 96: 846-851, 1999.
64. Michaels ML, Cruz C, Grollman AP, and Miller JH. Evidence that MutY and MutM combine to prevent mutations by an oxidatively damaged form of guanine in DNA. *Proc Natl Acad Sci U S A* 89: 7022-7025, 1992.
65. Morrow DA, and Givertz MM. Modulation of myocardial energetics: emerging evidence for a therapeutic target in cardiovascular disease. *Circulation* 112: 3218-3221, 2005.
66. Nascimben L, Ingwall JS, Lorell BH, Pinz I, Schultz V, Tornheim K, and Tian R. Mechanisms for increased glycolysis in the hypertrophied rat heart. *Hypertension* 44: 662-667, 2004.
67. Neely JR, Denton RM, England PJ, and Randle PJ. The effects of increased heart work on the tricarboxylate cycle and its interactions with glycolysis in the perfused rat heart. *BiochemJ* 128: 147-159, 1972.

68. Neely JR, Rovetto MJ, and Oram JF. Myocardial utilization of carbohydrate and lipids. *Prog Cardiovasc Dis* 15: 289-329, 1972.
69. Neubauer S, Horn M, Cramer M, Harre K, Newell JB, Peters W, Pabst T, Ertl G, Hahn D, Ingwall JS, and Kochsiek K. Myocardial phosphocreatine-to-ATP ratio is a predictor of mortality in patients with dilated cardiomyopathy. *Circulation* 96: 2190-2196, 1997.
70. Newsholme EA, and Randle PJ. Regulation of glucose uptake by muscle. 7. Effects of fatty acids, ketone bodies and pyruvate, and of alloxan-diabetes, starvation, hypophysectomy and adrenalectomy, on the concentrations of hexose phosphates, nucleotides and inorganic phosphate in perfused rat heart. *BiochemJ* 93: 641-651, 1964.
71. Nishioka K, Ohtsubo T, Oda H, Fujiwara T, Kang D, Sugimachi K, and Nakabeppu Y. Expression and differential intracellular localization of two major forms of human 8-oxoguanine DNA glycosylase encoded by alternatively spliced OGG1 mRNAs. *Mol Biol Cell* 10: 1637-1652, 1999.
72. Nojiri H, Shimizu T, Funakoshi M, Yamaguchi O, Zhou H, Kawakami S, Ohta Y, Sami M, Tachibana T, Ishikawa H, Kurosawa H, Kahn RC, Otsu K, and Shirasawa T. Oxidative stress causes heart failure with impaired mitochondrial respiration. *J Biol Chem* 281: 33789-33801, 2006.
73. Nuutila P, Maki M, Laine H, Knuuti MJ, Ruotsalainen U, Luotolahti M, Haaparanta M, Solin O, Jula A, Koivisto VA, and et al. Insulin action on heart and skeletal muscle glucose uptake in essential hypertension. *J Clin Invest* 96: 1003-1009, 1995.
74. Palaniswamy C, Mellana WM, Selvaraj DR, and Mohan D. Metabolic Modulation: A New Therapeutic Target in Treatment of Heart Failure. *Am J Ther* 2010.
75. Palmeira CM, Serrano J, Kuehl DW, and Wallace KB. Preferential oxidation of cardiac mitochondrial DNA following acute intoxication with doxorubicin. *Biochim Biophys Acta* 1321: 101-106, 1997.
76. Paz-Elizur T, Ben-Yosef R, Elinger D, Vexler A, Krupsky M, Berrebi A, Shani A, Schechtman E, Freedman L, and Livneh Z. Reduced repair of the oxidative 8-oxoguanine DNA damage and risk of head and neck cancer. *Cancer Res* 66: 11683-11689, 2006.
77. Paz-Elizur T, Krupsky M, Blumenstein S, Elinger D, Schechtman E, and Livneh Z. DNA repair activity for oxidative damage and risk of lung cancer. *J Natl Cancer Inst* 95: 1312-1319, 2003.
78. Pearce PC, Hawkey C, Symons C, and Olsen EG. Role of calcium in the induction of cardiac hypertrophy and myofibrillar disarray. Experimental studies of a possible cause of hypertrophic cardiomyopathy. *Br Heart J* 54: 420-427, 1985.

79. Pessin JE, and Bell GI. Mammalian facilitative glucose transporter family: structure and molecular regulation. *Annu Rev Physiol* 54: 911-930, 1992.
80. Radak Z, and Boldogh I. 8-Oxo-7,8-dihydroguanine: links to gene expression, aging, and defense against oxidative stress. *Free Radic Biol Med* 49: 587-596.
81. Ricci C, Pastukh V, Leonard J, Turrens J, Wilson G, Schaffer D, and Schaffer SW. Mitochondrial DNA damage triggers mitochondrial-superoxide generation and apoptosis. *Am J Physiol Cell Physiol* 294: C413-422, 2008.
82. Ritchie RH, Quinn JM, Cao AH, Drummond GR, Kaye DM, Favalaro JM, Proietto J, and Delbridge LM. The antioxidant tempol inhibits cardiac hypertrophy in the insulin-resistant GLUT4-deficient mouse in vivo. *J Mol Cell Cardiol* 42: 1119-1128, 2007.
83. Rutland C, Warner L, Thorpe A, Alibhai A, Robinson T, Shaw B, Layfield R, Brook JD, and Loughna S. Knockdown of alpha myosin heavy chain disrupts the cytoskeleton and leads to multiple defects during chick cardiogenesis. *J Anat* 214: 905-915, 2009.
84. Saddik M, and Lopaschuk GD. Myocardial triglyceride turnover and contribution to energy substrate utilization in isolated working rat hearts. *J Biol Chem* 266: 8162-8170, 1991.
85. Sadoshima J, Xu Y, Slayter HS, and Izumo S. Autocrine release of angiotensin II mediates stretch-induced hypertrophy of cardiac myocytes in vitro. *Cell* 75: 977-984, 1993.
86. Sauer U, Canonaco F, Heri S, Perrenoud A, and Fischer E. The soluble and membrane-bound transhydrogenases UdhA and PntAB have divergent functions in NADPH metabolism of Escherichia coli. *J Biol Chem* 279: 6613-6619, 2004.
87. Schwartz K, Boheler KR, de la BD, Lompre AM, and Mercadier JJ. Switches in cardiac muscle gene expression as a result of pressure and volume overload. *Am J Physiol* 262: R364-R369, 1992.
88. Serrano J, Palmeira CM, Kuehl DW, and Wallace KB. Cardiospecific and cumulative oxidation of mitochondrial DNA following subchronic doxorubicin administration. *Biochim Biophys Acta* 1411: 201-205, 1999.
89. Sheeran FL, Rydstrom J, Shakhparonov MI, Pestov NB, and Pepe S. Diminished NADPH transhydrogenase activity and mitochondrial redox regulation in human failing myocardium. *Biochim Biophys Acta* 1797: 1138-1148, 2010.
90. Shen W, Asai K, Uechi M, Mathier MA, Shannon RP, Vatner SF, and Ingwall JS. Progressive loss of myocardial ATP due to a loss of total purines during the development

of heart failure in dogs: a compensatory role for the parallel loss of creatine. *Circulation* 100: 2113-2118, 1999.

91. Shen X, Zheng S, Thongboonkerd V, Xu M, Pierce WM, Jr., Klein JB, and Epstein PN. Cardiac mitochondrial damage and biogenesis in a chronic model of type 1 diabetes. *Am J Physiol Endocrinol Metab* 287: E896-905, 2004.
92. Stanley WC, Recchia FA, and Lopaschuk GD. Myocardial substrate metabolism in the normal and failing heart. *Physiol Rev* 85: 1093-1129, 2005.
93. Stuart JA, Bourque BM, de Souza-Pinto NC, and Bohr VA. No evidence of mitochondrial respiratory dysfunction in OGG1-null mice deficient in removal of 8-oxodeoxyguanine from mitochondrial DNA. *Free Radic Biol Med* 38: 737-745, 2005.
94. Stubberfield CR, and Cohen GM. Interconversion of NAD(H) to NADP(H). A cellular response to quinone-induced oxidative stress in isolated hepatocytes. *Biochem Pharmacol* 38: 2631-2637, 1989.
95. Szczesny B, Hazra TK, Papaconstantinou J, Mitra S, and Boldogh I. Age-dependent deficiency in import of mitochondrial DNA glycosylases required for repair of oxidatively damaged bases. *Proc Natl Acad Sci U S A* 100: 10670-10675, 2003.
96. Taegtmeyer H, and Overturf ML. Effects of moderate hypertension on cardiac function and metabolism in the rabbit. *Hypertension* 11: 416-426, 1988.
97. Takimoto E, and Kass DA. Role of oxidative stress in cardiac hypertrophy and remodeling. *Hypertension* 49: 241-248, 2007.
98. Tanaka K, Honda M, and Takabatake T. Redox regulation of MAPK pathways and cardiac hypertrophy in adult rat cardiac myocyte. *J Am Coll Cardiol* 37: 676-685, 2001.
99. Tsutsui H. Oxidative stress in heart failure: the role of mitochondria. *Intern Med* 40: 1177-1182, 2001.
100. Tsutsui H, Kinugawa S, and Matsushima S. Mitochondrial oxidative stress and dysfunction in myocardial remodelling. *Cardiovasc Res* 81: 449-456, 2009.
101. van Bilsen M, van Nieuwenhoven FA, and van der Vusse GJ. Metabolic remodelling of the failing heart: beneficial or detrimental? *Cardiovasc Res* 81: 420-428, 2009.
102. van den Borne SW, Diez J, Blankesteyn WM, Verjans J, Hofstra L, and Narula J. Myocardial remodeling after infarction: the role of myofibroblasts. *Nat Rev Cardiol* 7: 30-37.

103. Van Houten B, Woshner V, and Santos JH. Role of mitochondrial DNA in toxic responses to oxidative stress. *DNA Repair (Amst)* 5: 145-152, 2006.
104. van Melle JP, Bot M, de Jonge P, de Boer RA, van Veldhuisen DJ, and Whooley MA. Diabetes, glycemic control, and new-onset heart failure in patients with stable coronary artery disease: data from the heart and soul study. *Diabetes Care* 33: 2084-2089, 2010.
105. Vogel R, Wiesinger H, Hamprecht B, and Dringen R. The regeneration of reduced glutathione in rat forebrain mitochondria identifies metabolic pathways providing the NADPH required. *Neurosci Lett* 275: 97-100, 1999.
106. Vogt AM, Elsasser A, Nef H, Bode C, Kubler W, and Schaper J. Increased glycolysis as protective adaptation of energy depleted, degenerating human hibernating myocardium. *Mol Cell Biochem* 242: 101-107, 2003.
107. Wang J, Song Y, Elsherif L, Song Z, Zhou G, Prabhu SD, Saari JT, and Cai L. Cardiac metallothionein induction plays the major role in the prevention of diabetic cardiomyopathy by zinc supplementation. *Circulation* 113: 544-554, 2006.
108. Wang Q, Donthi RV, Wang J, Lange AJ, Watson LJ, Jones SP, and Epstein PN. Cardiac phosphatase-deficient 6-phosphofructo-2-kinase/fructose-2,6-bisphosphatase increases glycolysis, hypertrophy, and myocyte resistance to hypoxia. *Am J Physiol Heart Circ Physiol* 294: H2889-2897, 2008.
109. Watson LJ, Facundo HT, Ngoh GA, Ameen M, Brainard RE, Lemma KM, Long BW, Prabhu SD, Xuan YT, and Jones SP. O-linked beta-N-acetylglucosamine transferase is indispensable in the failing heart. *Proc Natl Acad Sci U S A* 107: 17797-17802, 2010.
110. Weiss JN, and Lamp ST. Glycolysis preferentially inhibits ATP-sensitive K⁺ channels in isolated guinea pig cardiac myocytes. *Science* 238: 67-69, 1987.
111. Williamson DH, Lund P, and Krebs HA. The redox state of free nicotinamide-adenine dinucleotide in the cytoplasm and mitochondria of rat liver. *Biochem J* 103: 514-527, 1967.
112. Wu ML, and Vaughan-Jones RD. Effect of metabolic inhibitors and second messengers upon Na⁽⁺⁾-H⁺ exchange in the sheep cardiac Purkinje fibre. *J Physiol* 478 (Pt 2): 301-313, 1994.
113. Xu KY, Zweier JL, and Becker LC. Functional coupling between glycolysis and sarcoplasmic reticulum Ca²⁺ transport. *Circ Res* 77: 88-97, 1995.
114. Yakes FM, and Van Houten B. Mitochondrial DNA damage is more extensive and persists longer than nuclear DNA damage in human cells following oxidative stress. *Proc Natl Acad Sci U S A* 94: 514-519, 1997.

115. Yamazaki T, Komuro I, Kudoh S, Zou Y, Shiojima I, Hiroi Y, Mizuno T, Maemura K, Kurihara H, Aikawa R, Takano H, and Yazaki Y. Endothelin-1 is involved in mechanical stress-induced cardiomyocyte hypertrophy. *J Biol Chem* 271: 3221-3228, 1996.
116. Zerez CR, Lee SJ, and Tanaka KR. Spectrophotometric determination of oxidized and reduced pyridine nucleotides in erythrocytes using a single extraction procedure. *Anal Biochem* 164: 367-373, 1987.
117. Zhang J, Duncker DJ, Ya X, Zhang Y, Pavsek T, Wei H, Merkle H, Ugurbil K, From AH, and Bache RJ. Effect of left ventricular hypertrophy secondary to chronic pressure overload on transmural myocardial 2-deoxyglucose uptake. A ³¹P NMR spectroscopic study. *Circulation* 92: 1274-1283, 1995.

CURRICULUM VITAE

Jianxun Wang

Education:

- | | |
|------|--|
| 2011 | Ph.D. <i>Pharmacology and Toxicology</i> , University of
Louisville, School of Medicine, Department of
Pharmacology & Toxicology, Louisville, KY |
| 2007 | M.S. <i>Pharmacology and Toxicology</i> , University of
Louisville, School of Medicine, Department of,
Pharmacology & Toxicology, Louisville, KY |
| 1994 | M.S. <i>Genetics</i> , Sun Yat-sen University, Guangzhou,
China |
| 1991 | B.S., <i>Cell Biology</i> , Lanzhou University, Lanzhou, China |

Work and Research Experience:

- | | |
|-----------|--|
| 2003-2005 | Research associate, Division of
GastroenterologyHepatology,
Department of Medicine, University of Louisville |
| 2000-2003 | Research associate, Division of
Cardiology, Department of Medicine, University of
Louisville |

1994-2000	Instructor, Department of Central Laboratory, First Affiliated Hospital, Guangdong Medical College, Zhanjiang, China
2005-2011	Graduate Research Assistant, University of Louisville, School of Medicine, Department of Pharmacology & Toxicology Supervisor: Dr. Paul N. Epstein Thesis Title: “Cardiac abnormalities after transaortic constriction are worsened by changing glucose metabolism and benefited by repair of mitochondrial DNA”

Awards & Honors:

2005-2011	University Scholarship & Fellowship, University of Louisville
-----------	--

Peer reviewed Publications:

1. **Wang J**, Song Y, Elsherif L, Song Z, Zhou G, Prabhu SD, Saari JT, Cai L.
Cardiac metallothionein induction plays the major role in the prevention of
diabetic cardiomyopathy by zinc supplementation. *Circulation*. 2006 Jan
31;113(4):544-54. Epub 2006 Jan 23. PubMed PMID: 16432057.
2. **Wang J**, Song Y, Wang Q, Kralik PM, Epstein PN. Causes and characteristics of
diabetic cardiomyopathy. *Rev Diabet Stud*. 2006 Fall;3(3):108-17. Epub 2006 Nov
10. PubMed PMID: 17487334; PubMed Central PMCID: PMC1783586.

3. Song Y, **Wang J**, Li XK, Cai L. Zinc and the diabetic heart. *Biometals*. 2005 Aug;18(4):325-32. Review. PubMed PMID: 16158224.
4. Song Y, **Wang J**, Li Y, Du Y, Arteel GE, Saari JT, Kang YJ, Cai L. Cardiac metallothionein synthesis in streptozotocin-induced diabetic mice, and its protection against diabetes-induced cardiac injury. *Am J Pathol*. 2005 Jul;167(1):17-26. PubMed PMID: 15972948; PubMed Central PMCID: PMC1603431.
5. Cai L, **Wang J**, Li Y, Sun X, Wang L, Zhou Z, Kang YJ. Inhibition of superoxide generation and associated nitrosative damage is involved in metallothionein prevention of diabetic cardiomyopathy. *Diabetes*. 2005 Jun;54(6):1829-37. PubMed PMID: 15919806.
6. Wang Q, Donthi RV, **Wang J**, Lange AJ, Watson LJ, Jones SP, Epstein PN. Cardiac phosphatase-deficient 6-phosphofructo-2-kinase/fructose-2,6-bisphosphatase increases glycolysis, hypertrophy, and myocyte resistance to hypoxia. *Am J Physiol Heart Circ Physiol*. 2008 Jun;294(6):H2889-97. Epub 2008 May 2. PubMed PMID: 18456722.
7. Wang Y, Kodani E, **Wang J**, Zhang SX, Takano H, Tang XL, Bolli R. Cardioprotection during the final stage of the late phase of ischemic preconditioning is mediated by neuronal NO synthase in concert with cyclooxygenase-2. *Circ Res*. 2004 Jul 9;95(1):84-91. Epub 2004 May 27. PubMed PMID: 15166094.
8. Wang Y, Guo Y, Zhang SX, Wu WJ, **Wang J**, Bao W, Bolli R. Ischemic preconditioning upregulates inducible nitric oxide synthase in cardiac myocyte. *J Mol Cell Cardiol*. 2002 Jan;34(1):5-15. PubMed PMID: 11812160.

9. **Wang J**, Wang Q, Ye F. Genetic instability in cancer tissues analyzed by random amplified polymorphic DNA PCR. Chin Med J (Engl). 2002 Mar;115(3):430-2. PubMed PMID: 11940382.

Manuscripts in preparation:

1. Qianwen Wang , **Jianxun Wang** , and Paul N. Epstein Cardiomyocyte overexpression of kinase-active PFK-2 increases glucose oxidation despite decreased abundance and activity of pyruvate dehydrogenase complex
2. **Jianxun Wang** , Qianwen Wang , Lewis J. Watson , Steven P. Jones and Paul N. Epstein Cardiac overexpression of mitochondrial 8-oxoguanine DNA glycosylase 1 protects against cardiac fibrosis following transaortic constriction
3. **Jianxun Wang** , Qianwen Wang , Lewis J. Watson , Steven P. Jones and Paul N. Decreased glycolysis increases susceptibility to cardiac hypertrophy and heart failure
4. **Jianxun Wang** , Qianwen Wang , Lewis J. Watson , Steven P. Jones and Paul N. Increased glycolysis increases susceptibility to cardiac hypertrophy and heart failure